Journal of Zhejiang University-SCIENCE A (Applied Physics & Engineering) *2024 25(3):183-205*
www.jzus.zju.edu.cn; www.springer.com/journal/11582
E-mail: jzus_a@zju.edu.cn

Review

https://doi.org/10.1631/jzus.A2300457

Recent progress in the development of dielectric elastomer materials and their multilayer actuators

Shengchao JIANG[1,4], Junbo PENG[1,2,4], Lvting WANG[1,3], Hanzhi MA[1✉], Ye SHI[1✉]

[1]*ZJU-UIUC Institute, Zhejiang University, Jiaxing 314400, China*
[2]*College of Mechanical Engineering, Zhejiang University, Hangzhou 310058, China*
[3]*Department of Polymer Science and Engineering, Zhejiang University, Hangzhou 310058, China*
[4]*These authors contributed equally to this work*

Abstract: Dielectric elastomers (DEs) have emerged as one of the most promising artificial muscle technologies, due to their exceptional properties such as large actuation strain, fast response, high energy density, and flexible processibility for various configurations. Over the past two decades, researchers have been working on developing DE materials with improved properties and exploring innovative applications of dielectric elastomer actuators (DEAs). This review article focuses on two main topics: recent material innovation of DEs and development of multilayer stacking processes for DEAs, which are important to promoting commercialization of DEs. It begins by explaining the working principle of a DEA. Then, recently developed strategies for preparing new DE materials are introduced, including reducing mechanical stiffness, increasing dielectric permittivity, suppressing viscoelasticity loss, and mitigating electromechanical instability without pre-stretching. In the next section, different multilayer stacking methods for fabricating multilayer DEAs are discussed, including conventional dry stacking, wet stacking, a novel dry stacking method, and micro-fabrication-enabled stacking techniques. This review provides a comprehensive and up-to-date overview of recent developments in high-performance DE materials and multilayer stacking methods. It highlights the progress made in the field and also discusses potential future directions for further advancements.

Key words: Dielectric elastomer actuator (DEA); Dielectric elastomer (DE); Material synthesis; Multilayer stacking method

1 Introduction

Natural muscle is a unique material system that not only provides high energy density, but also can operate in a combination of modes with varying frequencies, strains, and cycles when stimulated with an electric pulse (Dickinson et al., 2000). Dielectric elastomers (DEs) have emerged as one of the most promising types of artificial muscle, owing to their compelling combination of large electrically induced actuation strain, high energy density, fast response speed, and mechanical compliancy, which reproduce—or in some aspects exceed—the multifunctional performance of natural muscles (Pelrine et al., 2000a; O'Halloran et al., 2008; Mirvakili and Hunter, 2018). Though the strain responses of dielectric materials under applied electric fields had been investigated since the late 18th century, studies on DEs and DE-based actuators rapidly increased only after 2000, when Pelrine et al. (2000a) reported actuation strains of DEs above 100%. This pioneering exploration has ignited enduring research enthusiasm concerning DE materials, actuator configurations, and their applications. Over the past two decades, researchers have extensively explored diverse material synthesis and processing methods, leading to the development of novel DE formulations and devices with substantially improved actuation performance (Romasanta et al., 2015; Guo YG et al., 2021; Guo YX et al., 2023; Tang et al., 2023).

When a thin film of DE is sandwiched by compliant electrodes, it works as a deformable capacitor known as a dielectric elastomer actuator (DEA) (Fig. 1). The application of an electric field generates electrostatic attraction between opposite charges, inducing a

✉ Ye SHI, yeshi@intl.zju.edu.cn
Hanzhi MA, mahanzhi@zju.edu.cn
Ye SHI, https://orcid.org/0000-0002-5228-1604

Received Sept. 6, 2023; Revision accepted Oct. 10, 2023;
Crosschecked Nov. 13, 2023; Online first Jan. 10, 2024

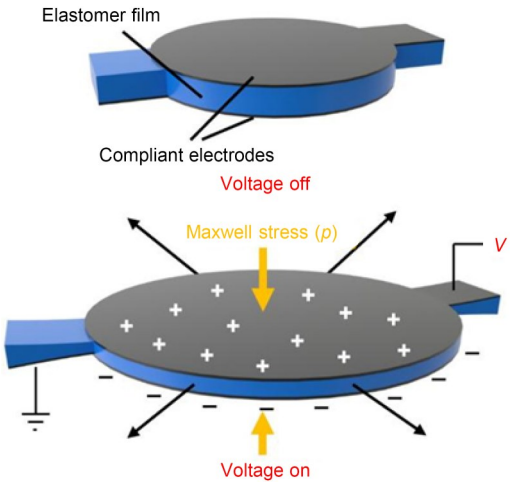

Fig. 1 Actuation mechanism of a DEA

pressure known as the Maxwell stress on the film. Consequently, the film undergoes compression in thickness and expansion in area, converting electrical energy into mechanical energy. The Maxwell stress is described as:

$$p=\varepsilon_0\varepsilon_r E^2=\varepsilon_0\varepsilon_r\left(\frac{V}{z}\right)^2, \tag{1}$$

where ε_r is the relative dielectric permittivity of the DE material, ε_0 is the permittivity of vacuum, E is the applied electric field, V is the applied voltage, and z is the film thickness. For strains below 20%, the change in thickness s_z can be defined by linear elasticity and free boundary approximations:

$$s_z=-\frac{p}{Y}=-\varepsilon_0\varepsilon_r\frac{E^2}{Y}, \tag{2}$$

where Y is the apparent elastic modulus of the DE at a certain actuation strain.

To evaluate the conversion of electrical energy to mechanical energy per unit volume of material in each cycle under a constant electric field, the electromechanical energy density (e) is often used, and is calculated as follows:

$$e=-0.5p\ln(1+s_z)=-0.5(\varepsilon_r\varepsilon_0E^2)\ln(1+s_z). \tag{3}$$

It is applicable for materials with non-linearity and high stretchability.

The equations above indicate that an ideal DE material is expected to have a large dielectric constant, high breakdown strength, high flexibility, and a proper stress–strain curve. However, few DE materials currently meet all the requirements above. As a result, one of the main focuses in the DE field over the past twenty years has been material innovation, which is also one of the main topics of this review. Currently, commercial DE materials such as 3M VHB™ tapes and silicone elastomers are widely used. However, VHB acrylic tapes suffer from response lag and high viscoelastic loss, while silicone elastomers are limited by exhibiting higher strain and are prone to dielectric breakdown under low electric field. Additionally, a long plateau in the stress–strain curve of these soft conventional elastomers is observed, and a failure mode known as electromechanical instability (EMI) limits their actuation performance. EMI occurs when a DE film is compressed below a certain thickness threshold. The Maxwell pressure keeps increasing and eventually gives rise to wrinkles or unstable snap-through. Traditional solutions to suppress EMI have been pre-stretching the elastomer film and maintaining the pre-strain with a rigid frame (Pelrine et al., 2000a). Researchers have developed various new DE materials including an interpenetrating polymer network (Ha et al., 2007), a bottlebrush elastomer (Vatankhah-Varnoosfaderani et al., 2017), an ultraviolet (UV)-cured all-silicone elastomer (Brochu et al., 2013), and a processable high-performance acrylate elastomer (Shi et al., 2022), to achieve better actuation performance and suppress EMI without the need for pre-stretching. In the next section, on development of DE materials, we will summarize recently developed strategies for material innovation of DEs, with a focused discussion of freestanding elastomers with inner pre-strain to suppress EMI.

In general, a high-performance DE should have a sufficiently high elastic strain, a large dielectric constant, a high dielectric strength, a high processing flexibility, and an actuation stability without EMI. However, the properties and performance of DE materials should be designed according to the intended application. For examples, DEs used to drive flying robots need to provide high power density and response speed, those applied for soft grippers should be able to output high forces, and those used to build peristaltic pumps should exhibit high actuation strain and driving bandwidth. We should also point out that different material-modification strategies usually have tradeoffs. For example, elastomers with low mechanical stiffness tend

to exhibit hysteresis and relaxation due to their inherent viscoelasticity, composite elastomers with higher dielectric permittivity usually have higher dielectric loss and lower dielectric strength, and low-viscoelasticity elastomers with plasticizer added can have stability issues. The advantages and disadvantages of different methods will be discussed in each sub-section.

Another key topic we discuss in this review is the development of multilayer DEAs (MDEAs), which is also a main focus in the DE field. Reducing the thickness of DE films is an effective way to decrease the driving voltage of DEAs, but it leads to reduced overall energy/force output and limited applications of DEAs. The MDEAs obtained by stacking single-layer DEAs in parallel improve robustness and guarantee force and energy outputs at low drive voltages. Thus, the development of MDEAs has attracted interest from many research groups, and different stacking methods and applications of MDEAs have been reported. In the section on multilayer stacking of DEAs, we will review recent progress in this area, including conventional dry stacking, wet stacking, a novel "dry-stacking" method recently reported by Shi et al. (2022), and other stacking methods based on microfabrication. We will summarize the salient aspects of these different multilayering processes and discuss their applications in DEA fabrication.

This review provides a detailed discussion of the recent innovation in DE materials, and thoroughly introduces important explorations on multilayer stacking methods over the past decades; it concludes with an outlook for future research trends.

2 Development of DE materials

From Eqs. (1)–(3), it is clear that actuation performance is largely dependent on a DE's intrinsic electro-mechanical properties, such as mechanical stiffness, dielectric permittivity, viscoelasticity, and stress–strain behavior. A DE with balanced electro-mechanical properties can potentially achieve high actuation strains with relatively low driving voltages, and thus avoid premature failure. Among a variety of off-the-shelf DE materials, acrylic-based VHB tapes and silicone elastomers are extensively used (Pelrine et al., 2000b). However, acrylic-based VHB tapes exhibit slow response speed and long-term relaxation due to their inherent viscoelasticity, and silicone elastomers have smaller actuation strain than that of VHB due to their higher mechanical stiffness and lower dielectric strength. Hence, researchers have been working on modifying DE properties either physically or chemically to provide balanced electromechanical performance. In this review, we primarily discuss the following strategies used to modify DE properties: (1) reducing mechanical stiffness, (2) increasing dielectric permittivity, (3) suppressing viscoelastic loss, and (4) suppressing EMI without pre-stretching.

2.1 Reducing mechanical stiffness

Reducing mechanical stiffness (lowering Young's modulus) of DEs has been demonstrated to be an effective way to enhance their actuation strain at lower driving voltages. Several strategies have been developed for this purpose. Löwe et al. (2005) first reported the effect of adding different plasticizers such as 81-R, 81-F, and 81-VF to a silicone elastomer to obtain low-modulus silicone elastomers. The addition of 5% plasticizer 81-R gave the lowest Young's modulus (0.35 MPa) and the highest area strain (10%) with an electric field of 32 V/μm, as tested on a circular planar actuator. Ni et al. (2020) developed a DE material with a low Young's modulus by introducing dioctyl phthalate (DOP) plasticizer into a natural rubber (NR) and $mTiO_2$/NR composite. The polar plasticizer DOP reduced entanglements among NR chains. As a result, Young's modulus was decreased from 0.89 to 0.49 MPa. The composite with added DOP exhibited an actuation strain of 25.3% under an electric field of 40 V/μm, which was 3.6 times that of the $mTiO_2$/NR composite without DOP. Nevertheless, these plasticizers are not stable and migrate easily, which affects the reliability of DE actuators.

Block polymers with soft segments have also been used for developing low-stiffness DEs. Zhang et al. (2018) synthesized an extremely soft DE composite with a colloidal blending strategy; it was a partially reduced graphene oxide (RGO)/polystyrene-*b*-poly(*n*-butyl acrylate)-*b*-polystyrene triblock copolymer (SBAS). The addition of 1.5% (mass fraction) reduced graphene oxide increased the modulus of SBAS from an original 0.30 to 0.51 MPa. However, the resulting DE composite was still very soft when compared to other commonly used DE composites such as pre-stretched VHB and silicones. While pure SBAS film

exhibited an actuation strain of 0.92% under an electric field of 7 V/μm, the actuation strain of 1.5% (mass fraction) RGO/SBAS composite film was increased to 3.51% under the same electric field. The 1.5% RGO/SBAS composite film free from pre-stretching attained the highest actuation strain of 21.30% at 33 V/μm.

Though reducing the mechanical stiffness of DEs can help improve actuation strain, it usually leads to stronger viscoelastic effects, lower force outputs, and lower breakdown strength.

2.2 Increasing dielectric permittivity

As expressed in Eq. (2), DEAs work as deformable capacitors; a higher dielectric permittivity corresponds to a greater capacitance, which reduces the electric field required for actuation. The dielectric permittivity is a measure of the electric polarizability of dielectrics, and it increases when the materials' polarizability increases (Fig. 2a). To enhance dielectric permittivity of DEs, two main approaches have been used: (1) chemical modification of an elastomer's polymeric network, and (2) development of elastomer composites. With regard to chemical modification, researchers have been focusing on introducing polar groups to a given elastomer network to achieve higher dielectric permittivity. Chemically modified elastomers are homogenous at the molecular level and have high dielectric strength. A number of polar groups have been introduced to polymer networks, such as nitrile, carbonate, sulfone, sulfonic esters, fluorine, chlorine, cyanopropyl, allyl cyanide group, and push-pull moieties such as nitroaniline. Dunki et al. (2015) synthesized a modified polymethyl-vinyl-siloxane (C2) via introduction of polar nitrile moieties, and it achieved a permittivity of about 10 at 1×10^4 Hz (Fig. 2b). The actuator fabricated with the synthesized elastomer had about 20% strain with a relatively low electric field of 10.8 V/μm. Recently, Sheima et al. (2023) synthesized an elastomer with a high permittivity (up to about 18) at 10 kHz by grafting polar sulfonyl side groups onto polymeric backbones (Figs. 2c and 2d). An actuator made with the synthesized elastomer showed the largest actuation strain of 14% under an electric field of 24.2 V/μm.

Development of elastomer composites by blending conductive fillers into the elastomer matrix is another common way of improving the dielectric permittivity of DE materials. Metal oxide fillers such as TiO_2 (Vudayagiri et al., 2014) and $BaTiO_3$ (Tang et al., 2005), and carbon-based conductive fillers such as

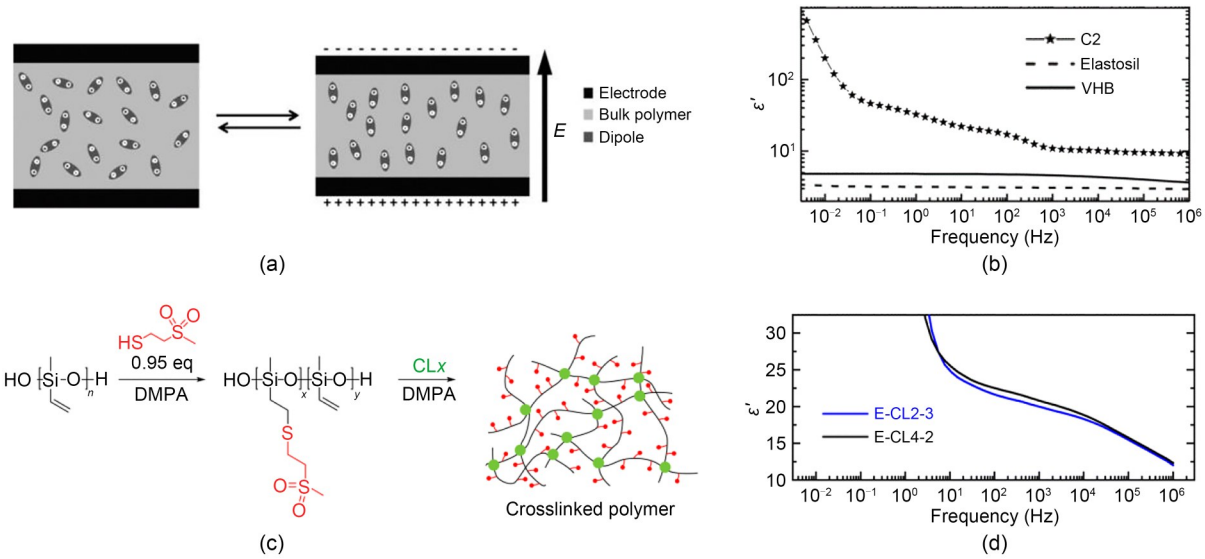

Fig. 2 (a) Schematic illustration of a DE carrying polar groups (the polar groups are oriented with their anode side to the anode side of the electrode and cathode side to the cathode side of the electrode) (reprinted from (Dünki et al., 2015), Copyright 2015, with permission from Wiley); (b) Permittivity at different frequencies of the synthesized elastomer (C2), Elastosil, and VHB (reprinted from (Dünki et al., 2015), Copyright 2015, with permission from Wiley); (c) Schematic illustration of grafting polar sulfonyl side groups onto polymeric backbones (DMPA represents 2,2-dimethoxy-2-phenylacetophenone) (reprinted from (Sheima et al., 2023), Copyright 2023, with permission from The Royal Society of Chemistry); (d) Permittivity at different frequencies of the synthesized elastomer (E-CL2-3, E-CL4-2) (reprinted from (Sheima et al., 2023), Copyright 2023, with permission from The Royal Society of Chemistry). ε' is the dielectric permittivity

carbon nanotubes (Galantini et al., 2013; Huang et al., 2022) and graphene layers (Romasanta et al., 2011), have been adopted for developing DE composites and been discussed in other review articles (Romasanta et al., 2015; Qiu et al., 2019; Suresh et al., 2023). Here, we mainly cover the ionic liquids (ILs) which are used as liquid conductive fillers and have been demonstrated to enhance DEs' dielectric permittivity without significantly stiffening them, as compared to solid fillers. Liu et al. (2019) synthesized high-permittivity DE materials by loading various ILs into a silicone elastomer, and found that 1-butyl-3-methylimidazolium hexafluoro antimonate ($BmimSbF_6$) showed the best results (Fig. 3a). The dielectric permittivity was more than 3 times higher than pristine silicone elastomer when 90 parts per hundred rubber (phr) $BmimSbF_6$ was loaded (Fig. 3b). Young's modulus of the synthesized elastomer also decreased as the amount of $BmimSbF_6$ increased. However, liquid fillers suffer from leakage problems that might lead to dielectric breakdown. To solve this problem, Wang et al. (2023) developed a solid-state stretchable poly(ionic liquid) (PIL) to greatly increase VHB's permittivity from 4.7 to 16.4 at 1 kHz, without increasing its stiffness (Fig. 3c). The PIL fillers were synthesized by photopolymerizing 1-hexyl-3-vinylimidazolium BF_4 (HVIM BF_4) and acetonitrile in precursor solution, and then encapsulating them in layers of VHB. Filler leakage was prevented by the strong interface formed between the VHB layers and PIL fillers due to ionic interaction between cations from polymer chains and mobile anions. The group tested planar actuators made with a PIL/VHB elastomer composite of varied PIL filler loadings, and the largest area actuation strain reached 133% under an electric field of 17 V/μm (Fig. 3d).

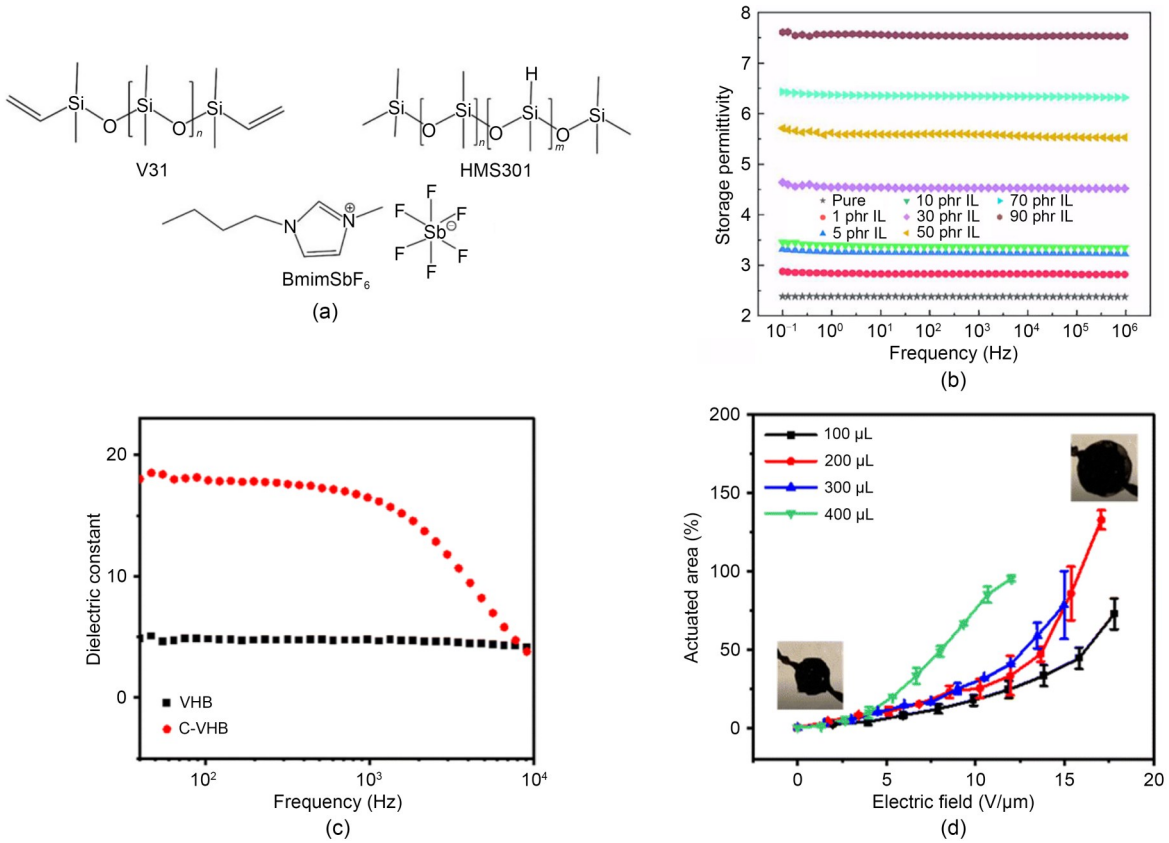

Fig. 3 (a) Chemical structures of polydimethylsiloxane (PDMS) (V31), a crosslinker (HMS301), and an IL ($BmimSbF_6$) (reprinted from (Liu et al., 2019), Copyright 2019, with permission from Wiley); (b) Storage permittivity curve of synthesized elastomers with different ionic liquid contents as a function of frequency (reprinted from (Liu et al., 2019), Copyright 2019, with permission from Wiley); (c) Permittivity as a function of the frequency of the elastomer composites PIL/VHB 4905 (C-VHB) and VHB (reprinted from (Wang et al., 2023), Copyright 2023, with permission from The Royal Society of Chemistry); (d) Actuated area strain as a function of the electric field of actuators with varied amounts of PILs (reprinted from (Wang et al., 2023), Copyright 2023, with permission from The Royal Society of Chemistry)

2.3 Suppressing viscoelastic loss

Polymers exhibit viscoelasticity due to the limited rotational freedom of polymer chains. High viscoelastic loss becomes an issue when DEs are driven at high frequencies, which leads to significantly reduced actuation strain due to viscous impedance. Hence, researchers have been working on developing strategies to suppress viscoelastic loss in DEs and improve their response speed. A common way to create low-viscoelasticity elastomers is adding a plasticizer into the polymer network, which can increase the free volume of polymer chains and promote their motion; however, this can result in stability issues because plasticizers are volatile and can evaporate during fabrication or usage of DEAs (Zhang et al., 2010; Azoug et al., 2014; Romasanta et al., 2015).

Recently, copolymers were synthesized with reduced viscoelasticity. Tan et al. (2019) modified the viscoelastic properties of a DE by copolymerizing polyurethane acrylate (PUA) with a polar crosslinker, low-molecular-weight polyethylene glycol diacrylate (PEGDA) (Fig. 4a). The addition of PEGDA minimized slippage of polymer chains and reduced hysteresis loss. A buckling-mode actuator was fabricated to test the actuation performance of this material, and the response time was demonstrated to decrease to below 1 s when the PEGDA concentration was increased to 10%–15% (mass fraction) (Fig. 4b). Yin et al. (2021) designed a polyacrylate DE (BAC2) and demonstrated a rotational motor apparatus fabricated with the designed elastomer material to prove the optimized attribute of rapid response. The elastomer was obtained by reacting macromolecular urethane acrylate with the monomer of *n*-butyl acrylate (*n*BA), as well as crosslinkers of polyether diol and aliphatic diisocyanate segments (Fig. 4c). The flexible chain segment of polyether diol acted as a lubricant in the polymer network and helped alleviate dipole-dipole interaction of poly(*n*BA). As a result, the response speed was enhanced and Young's modulus was lowered. An actuator fabricated with BAC2 exhibited 120% actuation strain after 400% biaxial pre-strain, almost 4 times the actuation strain of actuators made with commercialized VHB 4910 (Fig. 4d). From Fig. 4e, we can see that BAC2 had a less perturbed curve within the 1–100-Hz bandwidth than did VHB 4910, due to the suppressed mechanical loss.

2.4 Suppressing EMI without pre-stretching

Electromechanical instability, or the pull-in effect, is recognized as a main failure mode of DEs (Plante and Dubowsky, 2006), which leads to premature failure of DEs before high driving voltages are reached. Conventional soft DE materials usually show a long plateau in their stress–strain curves, during which the actuation stress–strain curve will intersect with it and trigger the pull-in effect (Fig. 5a). The reason is that at sufficiently high driving voltages, the reduction in film thickness and increase in electric field intensity form a positive feedback loop, which leads to unstable compression of the elastomeric material and ultimately, breakdown (Fig. 5b).

Pre-stretching has been found to be an effective method of suppressing EMI, and was first reported by Pelrine et al. (2000a). It shafts the origins of DEs' actuation stress–strain curve from point O to point O', thus avoiding the intersection of actuation and elastic stress–strain curves in the plateau region (Fig. 5a). The pre-stretching method is commonly used on silicone rubber and VHBs. The stretching ratio required to provide a feasible strain-stiffening effect in silicone rubber is smaller than that needed for a commercial acrylic VHB 4910 tape (Jiang et al., 2018).

During traditional pre-stretching, a rigid pre-strain-supporting structure is required to maintain the elastomer film, which adds load and volume to DEAs and may reduce the lifetime of devices (Fig. 6a). To overcome the drawbacks of this method, different strategies have been developed to synthesize freestanding polymers without the need for pre-stretching, including polymers with interpenetrating networks (IPNs), bottlebrush polymers, and bimodal networked polymers. Ha et al. (2007) developed an elastomer with an interpenetrating network by introducing and curing polymerizable and crosslinkable liquid additives into 400% pre-strained acrylic films. As Fig. 6b shows, a second network was formed within the acrylic elastomer host, which helped preserve a pre-strain of 245% after removal of the frame. The resulting film exhibited an actuation of 300% area strain and a breakdown strength of 420 MV/m. The interpenetrating network can be further modified by introducing additional functional components. For example, Han et al. (2023) reported a pre-strain-locked DE material named VHB-IPN-P, which was an interpenetrating network successfully built with a low Young's modulus (down

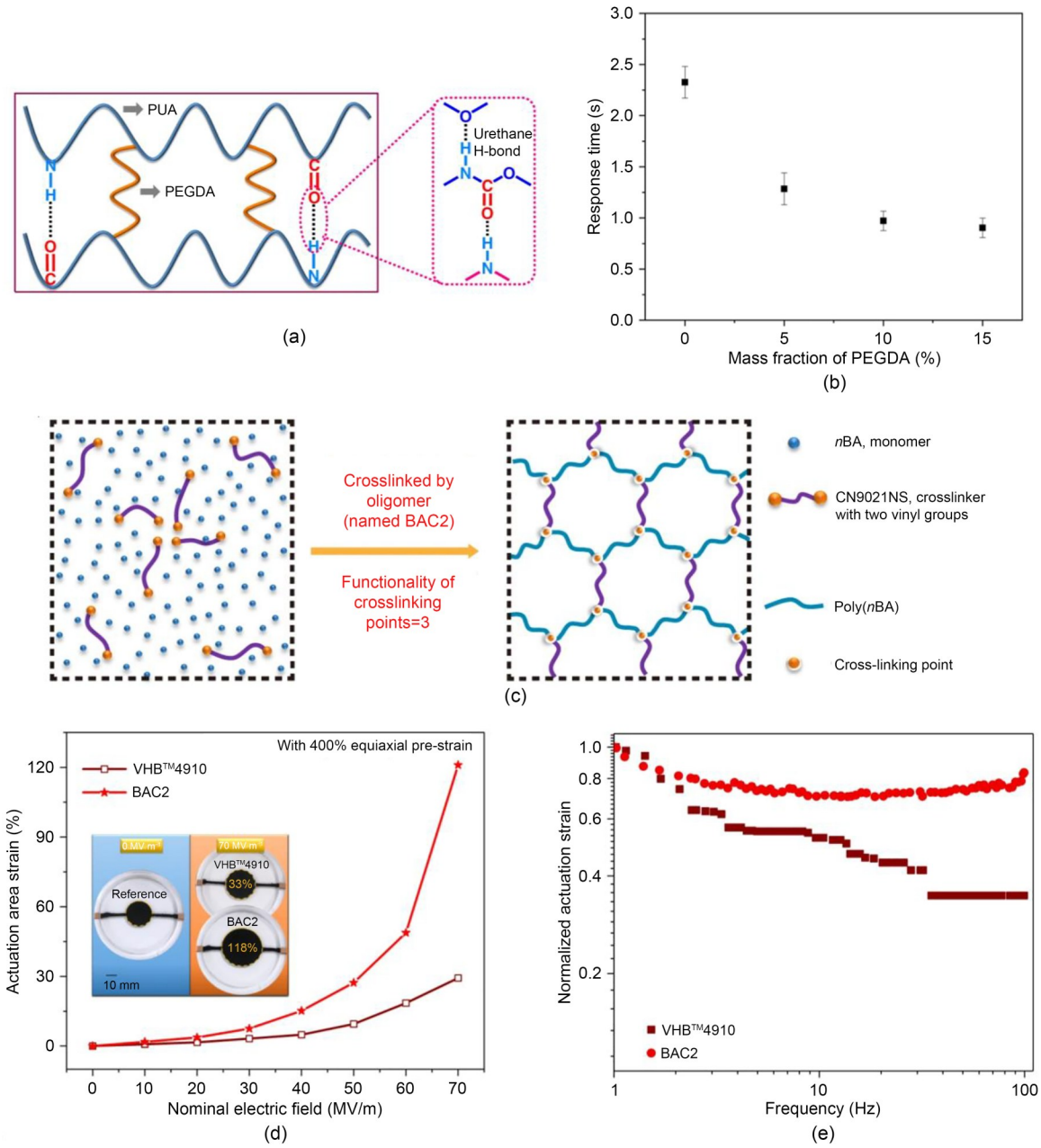

Fig. 4 (a) Schematic illustration of the crosslinking mechanism of PUA-PEGDA (reprinted from (Tan et al., 2019), Copyright 2019, with permission from Springer Nature); (b) Response time of a PEGDA actuator with different PEGDA concentrations (reprinted from (Tan et al., 2019), Copyright 2019, with permission from Springer Nature); (c) Schematic illustration of the mechanism of reacting macromolecular urethane acrylate with monomer of *n*BA and crosslinkers (reprinted from (Yin et al., 2021), Copyright 2021, with permission from Springer Nature); (d) Actuation area strains of VHB and BAC2 films with 400% biaxial pre-strain under varied electric field (reprinted from (Yin et al., 2021), Copyright 2021, with permission from Springer Nature); (e) Normalized actuation strain as a function of the frequency of VHB and the synthesized elastomer (BAC2) (driving voltage=5 kV) (reprinted from (Yin et al., 2021), Copyright 2021, with permission from Springer Nature)

to 0.48 MPa) achieved by introducing a second polymeric network and diffusing a plasticizer dibutoxyethoxyethyl formal (DBEF) into the VHB matrix (Fig. 6c). The prepared VHB-IPN-P film had a lower mechanical loss factor tanδ of 0.19 compared with that of VHB (about 0.8), and exhibited 185% actuation strain with an electric field of 66 V/μm. An actuator made with single-layer VHB-IPN-P material achieved an area strain

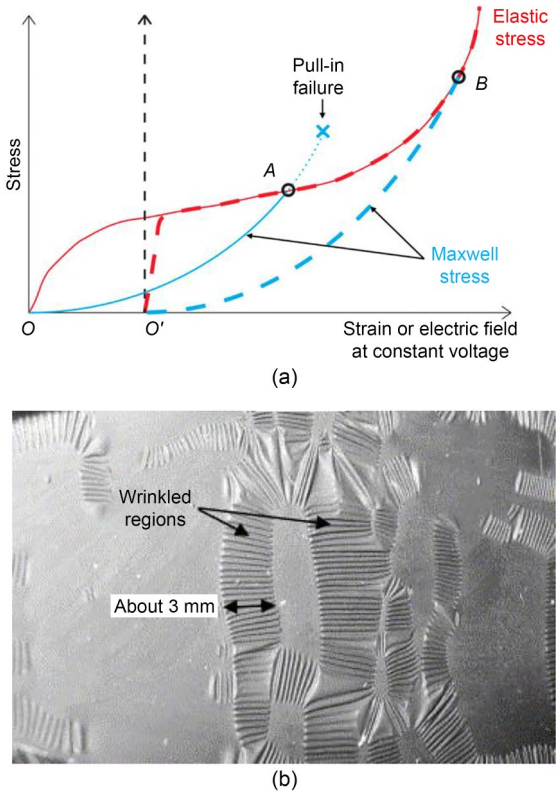

Fig. 5 (a) Stress–strain curve of DE films without pre-stretching enduring electromechanical instability (solid line) and stress–strain curve of pre-stretched DE films (dashed line) (dielectric breakdown occurred at point *A* and the breakdown strength could be valued at point *B*) (reprinted from (Qiu et al., 2019), Copyright 2019, with permission from ACS); (b) Film wrinkles generated by electromechanical instability (reprinted from (Plante and Dubowsky, 2006), Copyright 2006, with permission from Elsevier)

more than 175% at 0.1 Hz (Fig. 6d), and approximately 160% actuation strain was maintained when the frequency rose to 2.0 Hz.

Nevertheless, IPNs still require a pre-stretching and releasing process during the manufacture of elastomer films. Researchers have put effort into exploring DE materials that do not need a pre-stretching mechanism. Bottlebrush polymer was explored for its potential to suppress EMI without conventional pre-stretching due to its internal pre-strain. The first group to investigate it was Vatankhah-Varnoosfaderani et al. (2017). In the network of bottlebrush polymer, repeated side chains around the polymer main chains stretched the main chains and prevented them from entangling (Fig. 7a); thus, the bottlebrush polymer had a low Young's modulus at small strains. With increased strain, the polymer showed a strain-stiffening effect and the modulus increased to prevent dielectric breakdown. A DE film made with bottlebrush polymer exhibited strain larger than 300% under an electric field within 10 V/μm (Fig. 7b). Adeli et al. (2023) recently reported an on-demand crosslinkable bottlebrush polymer. A ring-opening metathesis polymerization was adopted to synthesize the bottlebrush polymer, while an efficient, environmentally friendly thiol-ene reaction was used to fabricate defect-free thin films. The synthesized bottlebrush polymer had double bonds around the backbone, which would be convenient for fast crosslinking into thin film and chemical modification with polar groups (Fig. 7c). With this material, free-stranding thin films with thickness below 100 μm gave up to 12% lateral actuation at 1000 V (Fig. 7d). The dielectric permittivity for a crosslinked bottlebrush polymer composite was increased to a value of 5.5 (Fig. 7e).

Strain-stiffening polymers have been also investigated because they could possibly eliminate EMI without a pre-stretching process. Niu et al. (2013) reported the synthesis of a UV-DE, which successfully eliminated EMI but exhibited a relatively low maximum area strain of less than 90% and suffered from high viscoelastic loss. Recently, Shi et al. (2022) developed a processable high-performance dielectric elastomer (PHDE) with bimodal-networked structure. The bimodal network was built using two crosslinkers with long chain segments (high molecular weight urethane diacrylate-CN9021) and short chain segments (propoxylated neopentyl glycol diacrylate-PNPDA). As Fig. 8a shows, the electromechanical instability of the bimodal network was suppressed compared with that of a conventional elastomer with a coiled network, owing to its strain-stiffening effect. The bimodal network enables a rapid increase in modulus after a critical stretch ratio, as the non-crystallizable elastomer is driven into its non-Gaussian region and begins to have stress redistribution (Fig. 8b). Furthermore, the introduction of hydrogen bonds by adding a comonomer of acid acrylate helped decrease the viscoelastic loss of the DE by increasing chain mobility within the elastomer network, while maintaining the stress–strain relationship. As shown in Fig. 8c, actuation tests showed that PHDE achieved a maximum area strain of about 190% under an electric field of 120 V/μm and a peak energy density of about 88 J/kg, with a 100-g load under a driving voltage of 2500 V (Fig. 8d); this was more than twice the strain of natural muscles. This PHDE synthesis

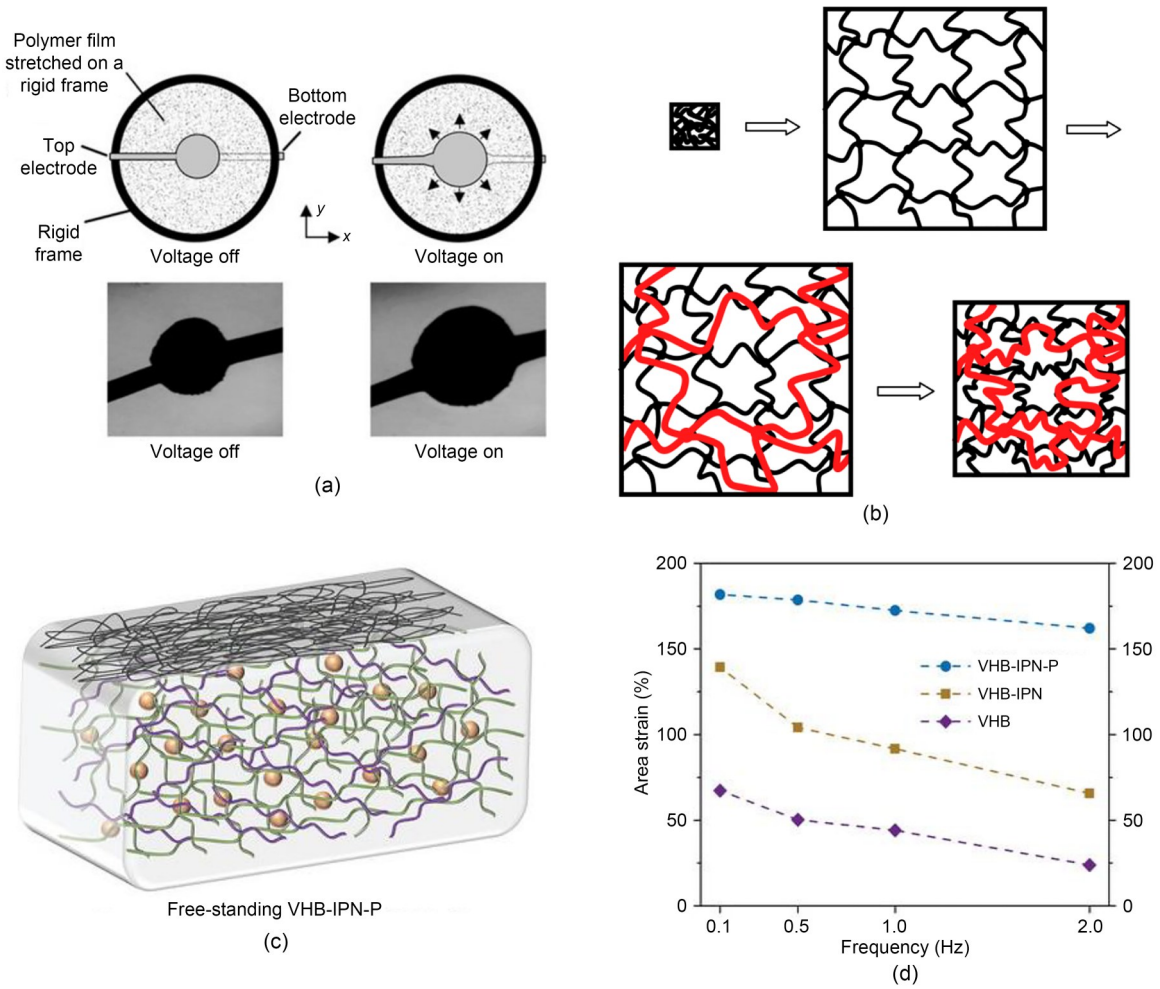

Fig. 6 (a) Pre-stretched VHB tape with rigid frame (reprinted from (Pelrine et al., 2000a), Copyright 2000, with permission from AAAS); (b) Schematic illustration of the formation of an interpenetrating polymer network (reprinted from (Ha et al., 2007), Copyright 2007, with permission from IOP Publishing); (c) Diagram form of the synthesized VHB-IPN-P polymeric network structure (reprinted from (Han et al., 2023), Copyright 2023, with permission from Wiley); (d) Area strain of VHB-IPN-P, VHB-IPN, and VHB as a function of different frequencies under 5-kV square-wave driving voltage (reprinted from (Han et al., 2023), Copyright 2023, with permission from Wiley)

may open the door for rational design of new DEs with mechanical and actuation properties tailored to meet specific application needs.

The mechanical properties and actuation performance of different DE materials are summarized in Table 1.

3 Multilayer stacking of DEAs

While scientists are working on the development of high-performance DE materials, many research groups in the DE community are also dedicated to developing multilayer stacking methods for MDEAs and new progress is continually reported. Due to the limitation of driving voltage, single-layer DEAs are usually made with thin films of thicknesses below 100 μm. As a result, the force and displacement outputs of single-layer DEAs are usually small and cannot meet the energy output requirements for practical application. Stacking multiple DEAs in parallel can scale up force and displacement outputs along the total number of layers without increasing the driving voltage. Early attempts at multilayer stacking (which are called conventional dry stacking methods here) physically adhere DE films together (Kovacs et al., 2009). Wet stacking methods—in which an uncured DE film is deposited on a cured DE—are being widely

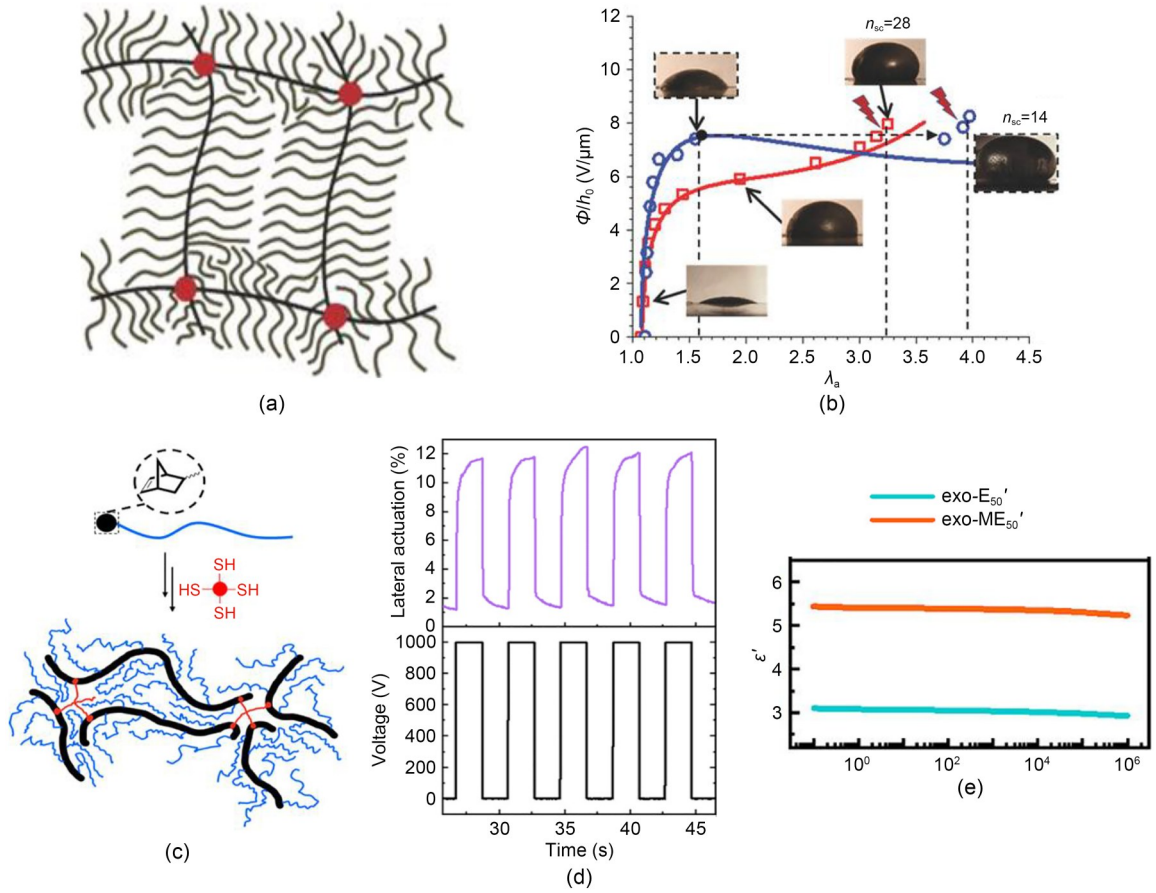

Fig. 7 (a) Schematic illustration of bottlebrush polymer network structure (reprinted from (Vatankhah-Varnoosfaderani et al., 2017), Copyright 2016, with permission from Wiley); (b) Actuation performance of two bottlebrush elastomer diaphragm actuators (network strand=200; side chain (n_{sc})=14, 28; λ_a is the areal expansion, Φ is the applied voltage, and h_0 is the elastomer film thickness; the dotted line stands for experimental data while the solid line stands for theoretical simulation results) (reprinted from (Vatankhah-Varnoosfaderani et al., 2017), Copyright 2016, with permission from Wiley); (c) Diagram of on-demand crosslinking bottlebrush polymer network structure (reprinted from (Adeli et al., 2023), Copyright 2023, with permission from ACS); (d) Cyclic actuation curve at 0.25 Hz of the exo-E$_{62}$′ (exo-E$_{62}$′ represents the bottlebrush polymer in which the molar concentration of the thiol group of the crosslinker to the mass of the polymer backbone is 62) 66-μm-thick bottlebrush polymer material (cyclic driving voltage=1000 V) (reprinted from (Adeli et al., 2023), Copyright 2023, with permission from ACS); (e) Dielectric permittivity as a function of the frequency of the exo-E$_{50}$′ and exo-ME$_{50}$′ bottlebrush polymer composite (exo-ME$_{50}$′ represents the polar group functionalized bottlebrush elastomers in which the molar concentration of the thiol group of the crosslinker to the mass of the polymer backbone is 50) (reprinted from (Adeli et al., 2023), Copyright 2023, with permission from ACS)

explored and applied for fabrication of MDEAs. Wet stacking methods can be categorized by the film casting method, for example spray-coating, blade-coating, or spin-coating. Recently, Shi et al. (2022) reported a novel dry stacking method with high efficiency and well-preserved actuation performance compared to single-layer counterparts. Micro-fabrication processes have also been introduced to build small-scale MDEAs. Here, we will review these multilayer stacking methods and discuss their advantages and drawbacks.

3.1 Conventional dry stacking methods

Conventional dry stacking methods for fabricating MDEAs have been reported in a few studies. Kovacs et al. (2009) reported MDEAs consisting of stacked 200–400 equally-sized single DE layers, produced with a pile-up strategy. The single DE film was coated with compliant electrode material, then multiple single DE film discs were stacked layer-by-layer in bottom-up serial configuration. The adjacent electrodes had alternating polarities to ensure electrical connection in

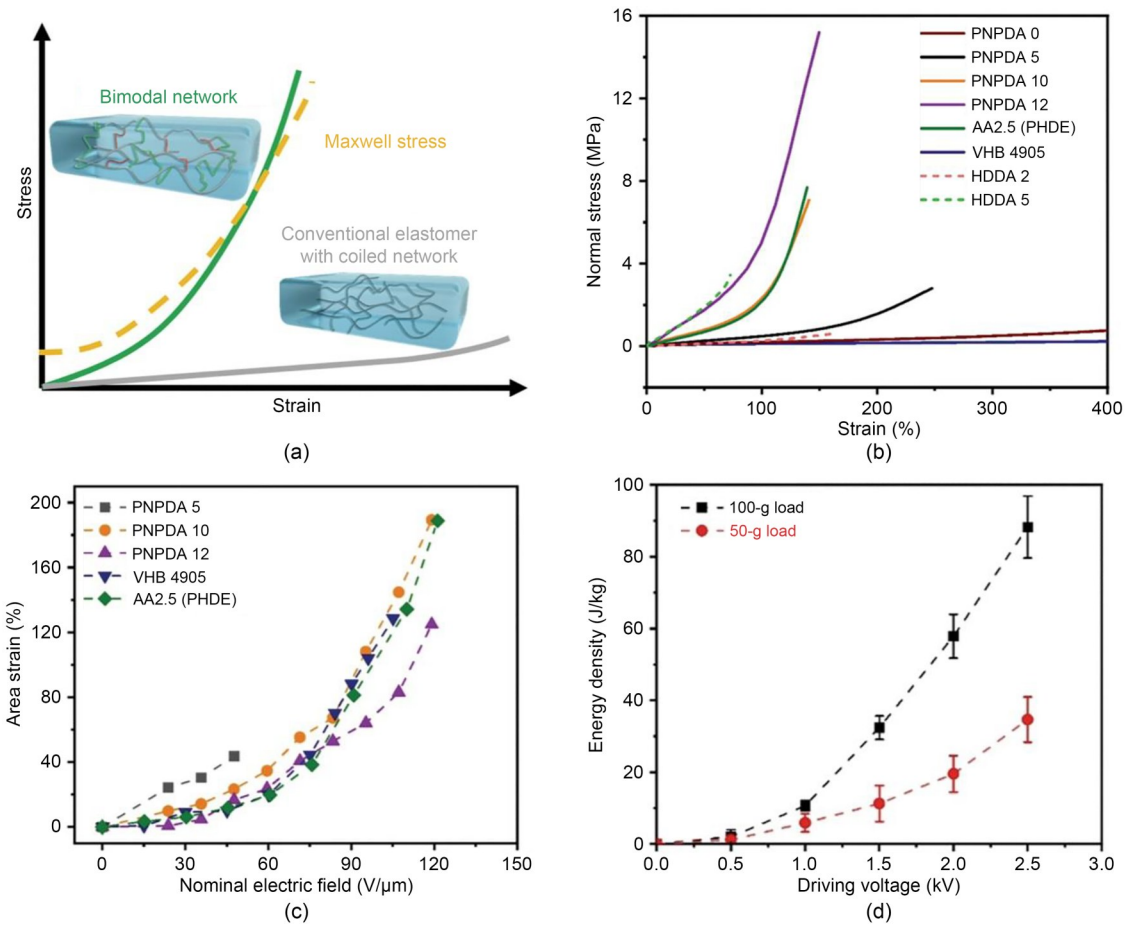

Fig. 8 (a) Bimodal network structure diagram and its stress–strain curve (green line) compared with conventional elastomer (grey line) (yellow dashed line stands for Maxwell stress curve as a function of strain); (b) Stress–strain curves of PHDE and VHB free from pre-stretching, and bimodal network elastomers with varied concentration of PNPDA/1,6-hexanediol diacrylate (HDDA); (c) Actuated area strain as a function of the electric field of diaphragm configuration actuators made of PHDE and VHB with 300% biaxial pre-stretching, and bimodal network acrylic elastomers with varied concentration of PNPDA; (d) Energy-density curve as a function of driving voltage of single-layer PHDE films with 100-g load and 50-g load. Reprinted from (Shi et al., 2022), Copyright 2022, with permission from AAAS. References to color refer to the online version of this figure

parallel (Fig. 9a). The 400-layer DEA showed approximately 10% linear contraction and the ability to lift approximately 2 kg of mass (Fig. 9b). The potential of DEAs to withstand and lift heavy loads was later reported by Tugui et al. (2019), who fabricated three versions of a 30-active-layer actuator using an elastomer designed in house (DET-Si-cb-30) and two commercialized elastomers (Elastosil-cb-30 and VHB-cb-30). To make multilayer actuators, carbon black powder was first coated on elastomer film and another dielectric layer was laminated on in the same way. Hand pressing was used after lamination to remove air bubbles between layers (Fig. 9c). The group compared actuation performance among these actuators. DET-Si-cb-30 actuator demonstrated superior actuation, lifting 250 times its own weight, while Elastosil-cb-30 lifted 220 times its weight, and VHB-cb-30 managed only 10 times its weight (Fig. 9d). Additionally, the DET-Si-cb-30 actuator exhibited a stable electromechanical response under a 5-kg load.

Because trapped air bubbles are a common issue during conventional dry stacking, the fabrication process was further modified to address this issue and thus improve the quality of MDEAs. Fu et al. (2022, 2023) reported a stack actuator with detachable and reconfigurable structure, produced through a fabrication process that combined the continuous spatial-confining network assembly (CSNA) electrode-fabrication method (Fu et al., 2022) with vacuum lamination (Fu et al., 2023). After transferring prepared electrodes onto pre-stretched

Table 1 Comparison of the mechanical properties and actuation performance of different DE materials

Strategy	DE	Pre-strain (x, y) (%)	Young's modulus (MPa)	Dielectric permittivity	Electric field (V/μm)	Maximum area strain (%)	Reference
Suppressing EMI with pre-stretching	Silicone rubber (Nusil CF19-2186)	(45, 45)	1	2.8@1 kHz	350	64	Pelrine et al., 2000a
	Silicone rubber (Dow Corning HS3)	(68, 68)	0.1	2.8@1 kHz	110	93	
	3M VHB 4910	(300, 300)	3	4.8@1 kHz	412	158	
	3M VHB 4910	(540, 75)	–	4.8@1 kHz	239	215	
Suppressing EMI without pre-stretching	VHB-poly (TMPTMA)	(400, 400)	~4	–	420	300	Ha et al., 2007
	VHB-IPN-P	(250, 250)	0.48	–	66	185	Han et al., 2023
	Bottlebrush polymer based on PDMS	–	–	–	<10	>300	Vatankhah-Varnoosfaderani et al., 2017
	exo-E_{62}'	–	0.019@10%	3.02@10 kHz	15	12	Adeli et al., 2023
	PHDE	–	1.3	5.35@1 kHz	120	189	Shi et al., 2022
Reducing mechanical stiffness	SR5 (5% 81-R/ silicone elastomer)	(40, 40)	0.35	3.25	32	10	Löwe et al., 2005
	50 phr DOP/ mTiO_2/NR	–	0.49	–	40	25.3	Ni et al., 2020
	1.5% RGO/SBAS	–	0.51	11@1 kHz	33	21.3	Zhang et al., 2018
Increasing dielectric permittivity	C2	–	0.154@10%	10.1@10 kHz	10.8	~20	Dünki et al., 2015
	E-CL2-3	–	0.628@10%	18.4@10 kHz	24.2	14	Sheima et al., 2023
	90 phr BmimSbF_6/ silicone elastomer	–	0.15	7.53@0.1 Hz	7.5*	–	Liu et al., 2019
	PIL/VHB 4905	(200, 200)	0.21	16.4@1 kHz	17	133	Wang et al., 2023
Suppressing viscoelastic loss	PUA-PEGDA-15	–	0.323@10%	9.4@1 kHz	24.2	71.4	Tan et al., 2019
	BAC2	(400, 400)	0.073	5.75@1 kHz	70	118	Yin et al., 2021

* Dielectric breakdown electric field

VHB elastomer film, the structure was moved to a vacuum freeze dryer to remove the air bubbles. Then, a new pre-stretched VHB elastomer film was attached on top and the process was repeated step by step until 9-layer-structure actuators were completed (Fig. 9e). The spring-roll actuator with 9-layer structure was successfully actuated, and achieved 3.1° of flexion under 7 kV in a lower-limb assistive device. The vacuum lamination process used in conventional stacking methods helped remove the air bubbles, ensure homogeneous distribution of electrical field (Fig. 9f), and improve the breakdown voltage (Fig. 9g).

However, DE layers stacked by conventional dry stacking methods are bonded together through the stickiness of films or van-de-Waals forces. As a result, these methods are only applicable for DEs with strong surface adhesion. DE films with low adhesion, such as silicone elastomers, cannot be stacked with these methods because the MDEAs are prone to breaking apart from tension creep when subjected to a tension load without voltage applied.

3.2 Wet stacking

Wet stacking is another widely used way for MDEA fabrication, during which the elastomer film and electrode are applied in a layer-by-layer manner. Wet stacking methods can be categorized by the film-casting method. Spray-coating is one effective way for wet stacking of DE films. Araromi et al. (2011) first reported a multilayer stacking process accomplished

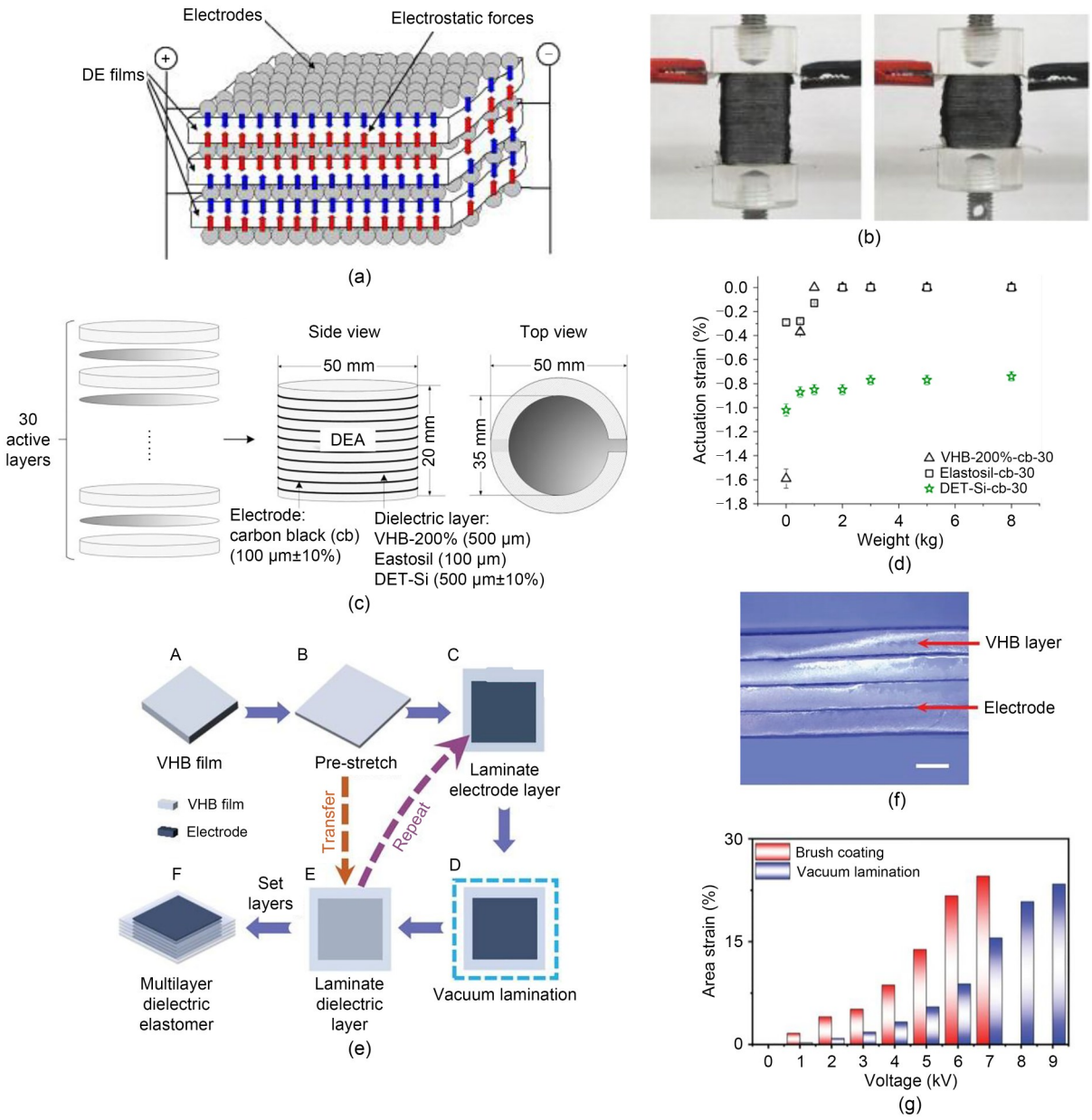

Fig. 9 MDEAs prepared by a dry stacking method: (a) layer-by-layer structure of multilayer stack actuators and (b) photos of a 400-layer stack actuator before and after electrical actuation (reprinted from (Kovacs et al., 2009), Copyright 2009, with permission from Elsevier); (c) schematic of a 30-layer DEA structure and (d) the actuation strain as a function of lifted weight for three MDEAs (VHB-200%-cb-30, Elastosil-cb-30, and DET-Si-cb-30) (reprinted from (Tugui et al., 2019), Copyright 2019, with permission from Elsevier); (e) fabrication process of MDEAs involving vacuum lamination (reprinted from (Fu et al., 2023), Copyright 2023, with permission from Wiley); (f) optical cross-sectional photo of an MDEA (reprinted from (Fu et al., 2023), Copyright 2023, with permission from Wiley); (g) actuated area strain as a function of driving voltage of actuators made with the traditional brush-coating process and a vacuum-lamination process (reprinted from (Fu et al., 2023), Copyright 2023, with permission from Wiley)

with a low-cost, consistently productive spray-deposition method. All the dielectric layers and electrodes layers were spray-deposited by a simple system composed of a direct-current (DC) motor, a wheel, and an air-brush system (Fig. 10a). However, the process had an extreme requirement for the fabrication environment. Small airborne particles had to be removed because they could decrease the layer thickness and the fabricated layers could be distorted by the particles (Fig. 10b). In addition, the electrode material, carbon grease, needed

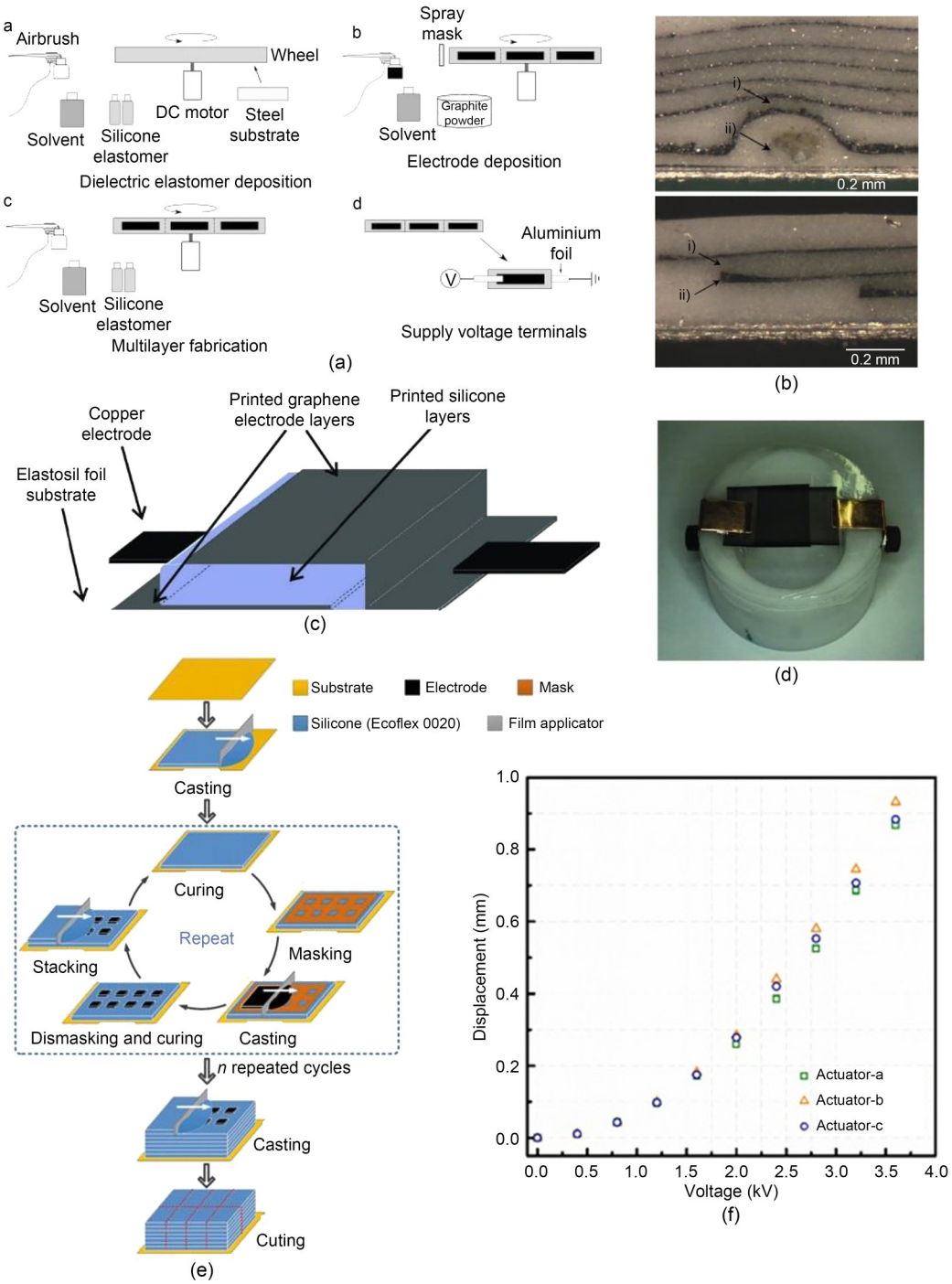

Fig. 10 A schematic diagram of MDEAs prepared by spraying dielectric and electrode layers with a DC motor (a) and cross-sectional photo of the contaminative part (above) and carbon-grease accumulation part (below) of a multilayer stack (b) (reprinted from (Araromi et al., 2011), Copyright 2011, with permission from Elsevier); Schematic representations of DEA (c) and MDEA (d) fabricated by aerosol-jet printing (reprinted from (Reitelshöfer et al., 2016), Copyright 2016, with permission from SPIE); Fabrication process of MDEAs involving blade-coating (e) and actuated displacement as a function of the driving voltage of three randomly chosen MDEAs (f) (reprinted from (Li et al., 2018), Copyright 2018, with permission from IOP Publishing)

to be extremely uniform. Any accumulation of carbon grease could cause dielectric breakdown at lower voltages (Fig. 10b). Reitelshöfer et al. (2016) introduced an aerosol-jet-printing process to print a fully

functional 2-layer stacked DEA (Figs. 10c and 10d). The aerosol-jet-printing system was composed of two atomizers, virtual impactors, and printing nozzles. The fabricated film (under 20 μm) was relatively homogenous when the printing-nozzle movement patterns were improved.

To efficiently prepare large-area DE films and stacks, film-casting methods such as blade-coating and slot-die coating have been also adopted for wet stacking processes. Li et al. (2018) fabricated a stacked DEA via blade-coating, which involved three main steps: (1) blade-coating a silicone encapsulation layer on polyethylene terephthalate (PET) substrate, (2) placing a shaped mask on the silicone layer and blade-coating the liquid electrode material over it, and (3) coating the actuation layer on (Fig. 10e). Three randomly chosen stacked dielectric elastomer actuators (SDEAs) showed similar voltage-contraction curves, which indicated that the fabricated SDEAs maintained reproducible properties (Fig. 10f). Iacob et al. (2022) recently reported a slot-die coating method to make MDEAs, using an optimized nitrile-butadiene rubber (NBR). Fig. 11a shows how a 50-layer MDEA was made by compiling 10 small 5-layer A2 stack actuators together; the enlarged image shows the consistency in dielectric layer thickness, which was about 160 μm. The 50-layer MDEA exhibited an actuation strain of 0.3% under a driving voltage of 2500 V (Fig. 11b). Danner et al. (2022) reported an environmentally friendly, solvent-free multilayer stack-fabrication method based on blade printing, and fabricated the multilayer stack actuator by a green process. The silicone composites were synthesized via in situ polymerization of cyclosiloxane monomers, with graphene nanoplatelets added. Then, the synthesized homogenous composite was screen-printed to electrodes and crosslinked under 110 ℃ (Fig. 11c). The electrode material was screen-printed three times to guarantee that the electrode was fully and uniformly covered on the silicone composite layer. MDEAs were made by repeating these steps. The whole fabrication process was free from any solvents. The 50-layer actuator exhibited reversible actuation under driving voltage, up to 5700 V (Figs. 11d and 11e).

Spin-coating is another commonly used film-preparation method for wet stacking, since the instrument is available to most labs and the film thickness can be tuned by controlling the spin speed. Duduta et al. (2016) reported a successful manufacturing process that achieved spin-coating for MDEAs using a CN9021-based elastomer precursor (Fig. 12a). The cross-sectional image of the multilayer structure demonstrated the uniformity of the single-layer thickness (Fig. 12b). Duduta et al. (2019) fabricated a multilayer linear contracting actuator with large force outputs by combining the previously reported spin-coating method and a physical stacking method. The 1170-layer actuator was able to lift a load of 1 kg by 8 mm under a driving voltage of 3 kV (Fig. 12c). It exhibited a high energy density of about 20 J/kg under an electric field over 100 V/μm, which was comparable to that of natural muscle (Fig. 12d). Ren et al. (2022) modified the spin-coating process to shorten fabrication time and improve the scalability of manufacturing. An extra post-transfer baking step was added after the carbon nanotube (CNT) transfer step to remove as much surfactant as possible, thus lessening the curing time of the last dielectric layer (Fig. 12e). A vacuum lamination step was also used to ensure more uniform thickness of the dielectric layers and eliminate air bubbles, which helped increase dielectric strength (Fig. 12e). MDEAs fabricated by spin-coating have been tested in various applications. Chen et al. (2019) reported a flying robot with high energy density, in which the driving DEA was prepared using a commercially available elastomer and the spin-coating method. To attain sufficient power density (>200 W/kg) to lift up the soft actuators, a pre-stretch-free multilayer rolled DEA with a power density of 600 W/kg was fabricated, and the power density was increased by stacking seven dielectric layers and six CNT electrode layers (Fig. 12f). Hajiesmaili and Clarke (2019) demonstrated that MDEAs prepared by spin-coating could change their shape through Gaussian curvature variation and control a specified actuation area (Fig. 12g). A more sophisticated shape-changing mechanism was presented recently by Hajiesmaili et al. (2022), which realized successful area-controlled actuation into the target shape of a human face profile.

3.3 A novel dry stacking method

Wet stacking methods are time-consuming and low-yield because the film casting, film curing, and electrode deposition steps are conducted sequentially. They can also be compounded by issues from film-casting methods which are amplified when coating a soft DE film with an uneven surface (patterned electrodes).

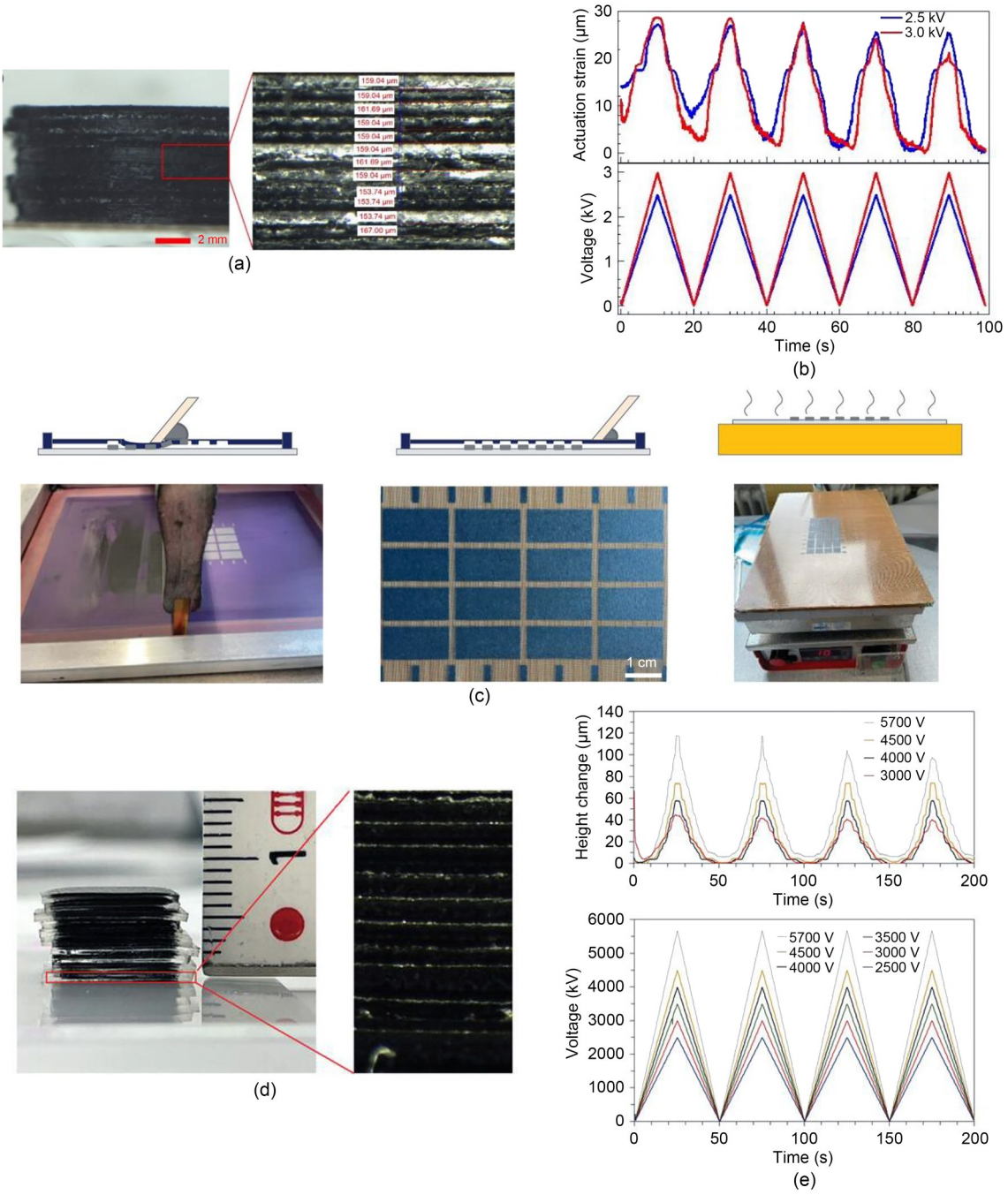

Fig. 11 Cross-sectional picture (a) and actuation-strain curve and corresponding cyclic voltage curve as a function of time of the MDEAs (b) (reprinted from (Iacob et al., 2022), Copyright 2022, with permission from ACS); Screen-printing the composite to electrodes and crosslinking at 110 ℃ (c); Cross-sectional photo (d) and actuated displacement curve and corresponding voltage curve as a function of time of MDEAs (e) (reprinted from (Danner et al., 2022), Copyright 2022, with permission from Wiley). References to color refer to the online version of this figure

Film defects formed due to air-borne particles or trapped air bubbles cannot be avoided during fabrication of DE films. In dry stacking processes, however, any DE layer with visible defects can be replaced with a pristine layer prior to stacking. Furthermore, the wet stacking methods are not suitable for pre-formed films like VHB tapes because such films are not suitable for layer-by-layer processing.

Shi et al. (2022) reported a novel dry stacking method that achieved high efficiency and yield during

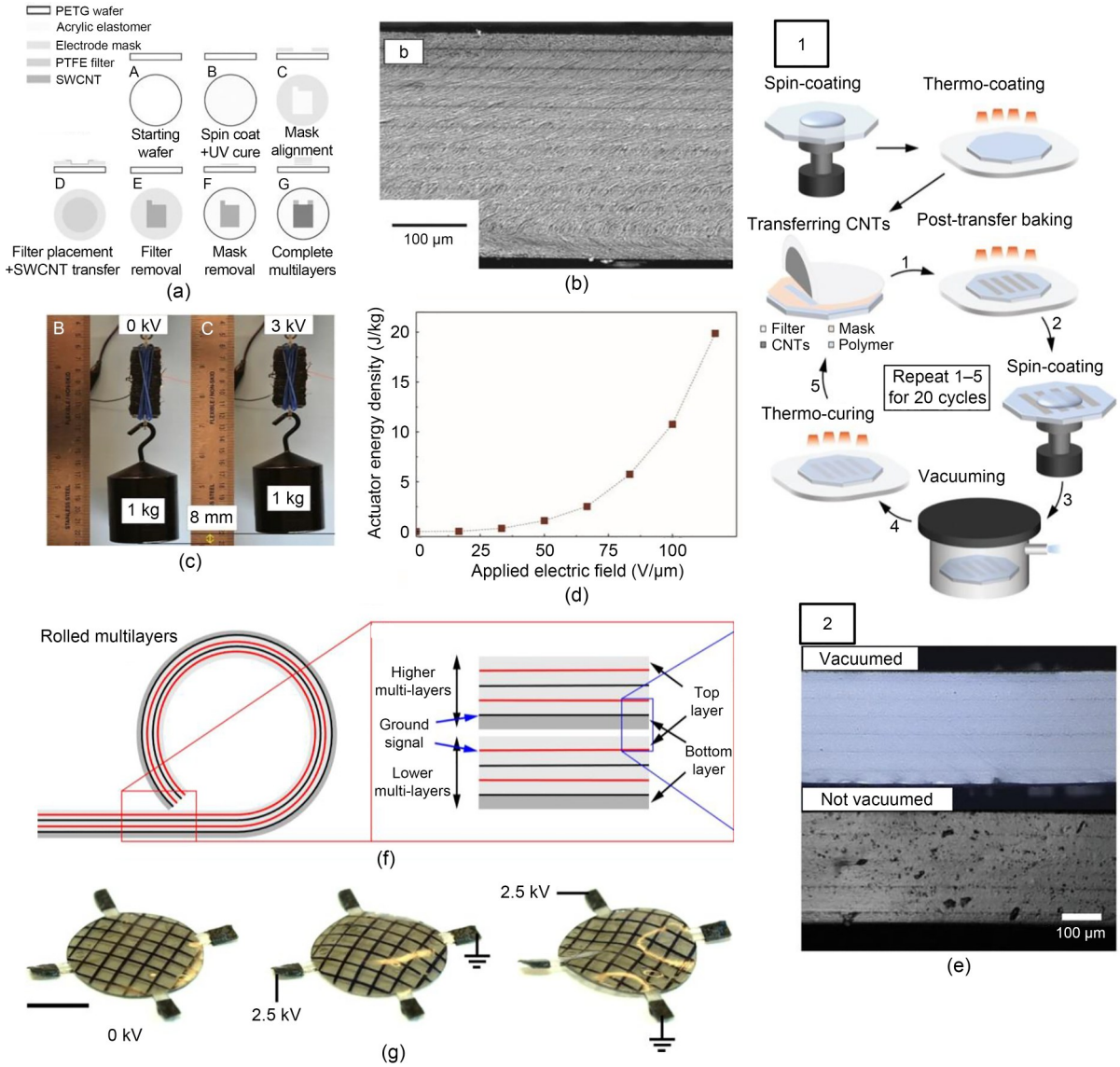

Fig. 12 Fabrication process of MDEAs (a) and cross-sectional microscopy image of a 12-layer stack (b) (PETG represents the polyethylene terephthalate glycol, PTFE represents the polytetrafluoroethylene, and SWCNT represents the single-walled carbon nanotube) (reprinted from (Duduta et al., 2016), Copyright 2016, with permission from Wiley); Optical picture of an MDEA lifting a load of 1 kg under 3 kV (c); Actuator energy density as a function of electric field of MDEAs (d) (reprinted from (Duduta et al., 2019), Copyright 2019, with permission from National Academy of Science, the USA); Fabrication process of MDEAs involving vacuum lamination (1) and scanning electron microscope (SEM) images of the cross-sectional part of DEAs fabricated with or without vacuum lamination (2) (e) (reprinted from (Ren et al., 2022), Copyright 2022, with permission from Wiley); Schematic of rolled MDEAs (f) (reprinted from (Chen et al., 2019), Copyright 2019, with permission from Springer Nature); An initially flat MDEA exhibiting reconfiguration under a driving voltage of 2.5 kV (g) (reprinted from (Hajiesmaili et al., 2019), Copyright 2019, with permission from Springer Nature)

fabrication (Fig. 13a). They fabricated PHDE MDEAs using this method. In a typical manufacturing process, a single PHDE film was prepared on a PET substrate while the remaining PHDE films were cast on cleaned pieces of glasses. The pieces of glasses with PHDE films were sprayed with CNT electrodes and a binding layer composed of uncured acrylic-polymer precursor. Then, the PET/PHDE was aligned on a glass/PHDE/CNT/precursor and laminated. The glass was removed after the precursor layer was UV cured, and the PET part with two-layer PHDE was stacked onto another piece of glass with PHDE film. The final multilayer PHDE stack was manufactured by repeating the steps above.

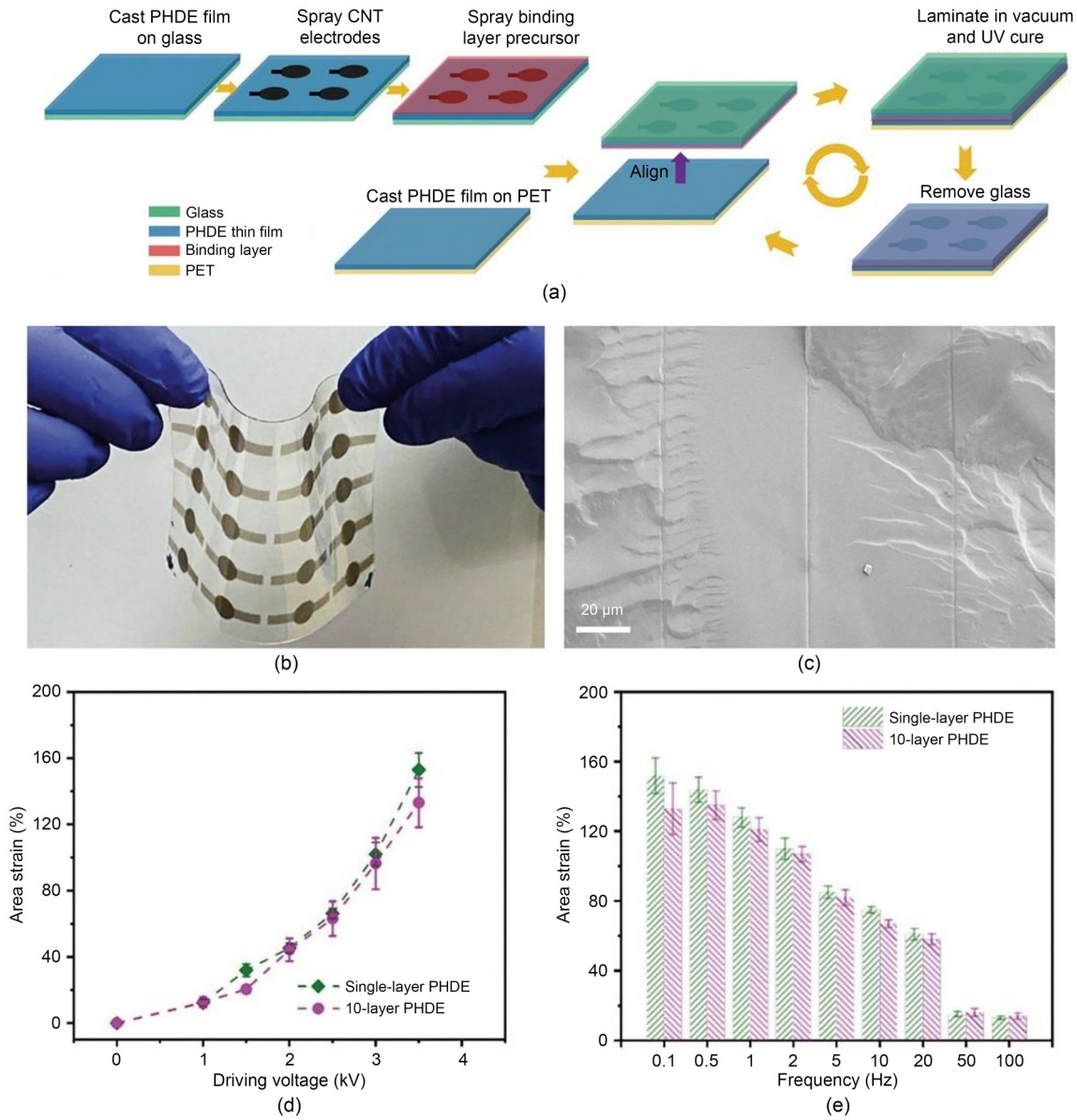

Fig. 13 Fabrication process of a multilayer PHDE actuator (a); Optical image (b) and cross-sectional SEM image (c) of PHDE MDEAs; Area strain curve as a function of driving voltage (d) and frequency (e) of single-layer PHDE actuators and 10-layer PHDE actuators. Reprinted from (Shi et al., 2022), Copyright 2022, with permission from AAAS

This novel dry stacking method is more compatible with large-scale fabrication than wet stacking methods that use a layer-by-layer process. The thickness of DE films could be easily tuned by controlling film-fabrication methods, such as blade-coating, slot-die coating, or roll-to-roll fabrication. Furthermore, the film quality was guaranteed by pre-screening cured single layers to check any defects or non-uniformity and substitute an imperfect layer with a new one if necessary (Figs. 13b and 13c). Higher fabrication efficiency was attained by casting PHDE films with electrodes at the same time and using a modular stacking process. From Fig. 13d, one can see that a 10-layer PHDE stack actuator showed a similar actuation strain trend under a rising driving voltage to that of a single-layer film actuator. In addition, the multilayer actuator exhibited high response speed, as about 90% of the actuation strain was maintained after the driving frequency was increased from 0.1 to 2.0 Hz (Fig. 13e).

This novel dry stacking method achieved strong bonding between DE layers. The electrodes are applied by forming an ultrathin, highly compliant, and

conductive CNT network on the DE surface. This is followed by infiltrating a rubbery polymer precursor into the CNT network. This new interfacial electrode with interpenetrating structure can seal/protect the CNT network and glue the adjacent DE polymer layers. This method is also highly compatible with different DE materials, but the material used for the adhesion layer should be carefully selected. It has been used for uncured films such as PHDE and silicones, as well as for pre-formed films such as pre-stretched VHBs and IPNs (Han et al., 2023).

3.4 MDEAs fabricated by micro-fabrication

There are several reports on emerging multilayer fabrication processes that adopt micro-fabrication. Among them, 3D printing has received extensive attention in fabricating DEAs due to the rapid prototyping, custom design, and one-step fabrication of complex structures that it offers (Zolfagharian et al., 2016). Chortos et al. (2020) fabricated 3D MDEAs by 3D printing interdigitated vertical electrodes and then filling and curing the DE precursor solution (Fig. 14a). The fabricated actuator exhibited in-plane shrinkage strain of up to 9% at 25 V/μm. This proved the feasibility of involving 3D printing technology in MDEA manufacturing. However, the current 3D printing technology only prints a single-component material and cannot realize integrated molding of MDEAs. Therefore, we await advances in sophisticated 3D printing technology that would be suitable for fabricating MDEAs.

Recently, several research groups have reported breakthroughs in 3D printing of MDEAs. Palmić and Slavič (2022) presented the first-ever demonstration of monolithically 3D-printed stacked dielectric actuators using a single fabrication process, with a commercially available extrusion 3D printer and thermoplastic filaments. To address the issue of uneven printed surfaces in the fused-filament-fabrication (FFF) 3D-printing process, the pair proposed two effective strategies—designing a customized G-code generation program to achieve separate specification of process parameters and deposition strategies for each region of an MDEA, and ironing the surface of each electrode and dielectric layer to flatten them to a specified height (Fig. 14b). However, the actuation performance of the MDEAs was still limited by the thick electrode layer. Su et al. (2023) presented a 3D printing fabrication process which showed advantages in fabrication efficiency and maintained similar actuation performance to that of actuators made by spin-coating. A novel printing method was used to cure the boundary of the printed layer and then the ink tank was filled with DE ink; printing was delayed for 2–5 s before UV curing, which effectively reduced internal structural defects and improved surface smoothness (Figs. 14c–14e). However, the main problem with this 3D printing process was that it was hard to print DE films with thicknesses below 50 μm.

Meanwhile, Son et al. (2023) fabricated a lateral MDEA with photolithography and secondary sputtering (Fig. 14f). This method can form a pre-designed electrode structure on the microscale and eventually form stacked DEAs. The single-cycle process of fabricating an MDEA with regular spacing and size greatly improved efficiency. However, large-scale and high-performance MDEAs cannot be prepared via this method due to the limitations of the expensive instrument such as photolithography and secondary sputtering, as well as the interdigitated polymer frame (SU-8) within MDEAs. We expect that in the future, further development in micro-fabrication technology and utilization of different facilities will optimize either the fabrication process or the actuation performance.

4 Conclusions and outlook

DEs exhibit a unique combination of light weight, large strain, high energy density, fast response, and exceptional mechanical compliance, making them a favorable material for a wide range of applications such as soft robots, haptic interactions, and wearable devices. To further improve DEs' properties and promote their practical application, researchers have been working on developing new DE materials. Strategies for reducing stiffness, increasing dielectric permittivity, and suppressing viscoelasticity loss have been developed to improve the actuation performance of DEs. Recently, DE materials which successfully suppress EMI without the need for pre-stretching have been synthesized. They provide both high performance and processability, thus paving the way for the commercialization of DEA devices with different configurations.

However, several issues still need to be addressed before DEs can be widely used in commercial applications. Firstly, designing DE materials which can maintain large and stable actuation strain (over 100%) under

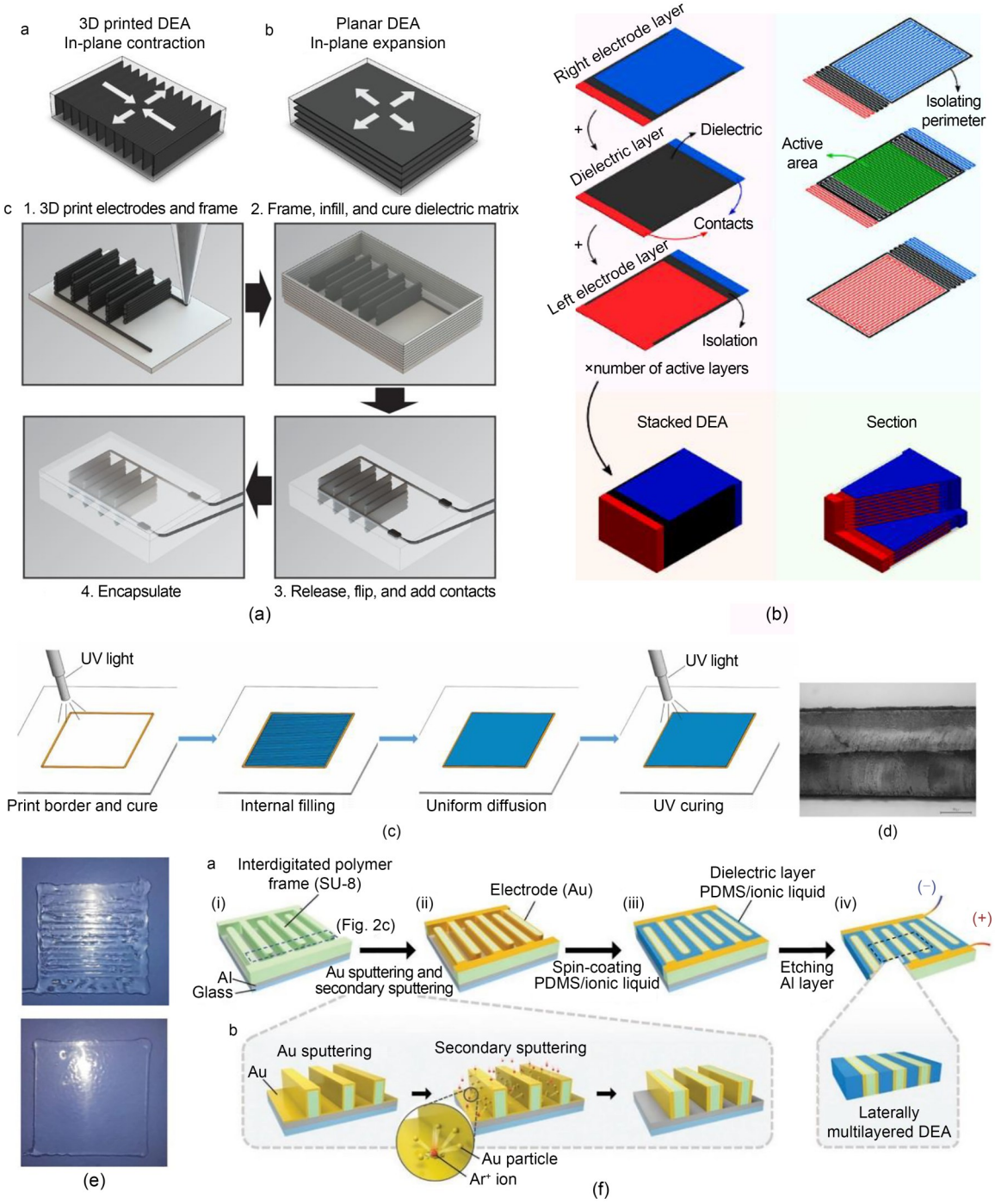

Fig. 14 (a) Schematic illustration of a 3D printing process for MDEAs with vertical/horizontal/interdigitated electrodes (reprinted from (Chortos et al., 2020), Copyright 2019, with permission from Wiley); (b) Illustration of SDEA fabrication (reprinted from (Palmić and Slavič, 2022), Copyright 2022, with permission from Elsevier); (c) Schematic illustration of the improved printing process; (d) Cross-sectional SEM photo of the printed layers; (e) Optical images of printed samples printed with an unimproved or improved print path (reprinted from (Su et al., 2023), Copyright 2023, with permission from Wiley); (f) Schematic of the preparation process of an MDEA with electrode fabrication details added via a secondary sputtering process (reprinted from (Son et al., 2023), Copyright 2023, with permission from Wiley)

high driving frequencies (on the order of 100 Hz) still remains a challenge. The modification of network structures and development of composites based on acrylics are possible ways of preparing DE materials

with both high strain and broad bandwidth. Secondly, the long-term stability of DEs and DEAs remains a concern. Different mechanisms that occur during long-term cyclic operations, such as charge accumulation and heat generation, can cause premature electrical breakdown of weak areas in DEAs. To improve lifetime, failure mechanisms should be carefully studied and the dielectric properties of DE materials should be properly tailored based on the mechanisms. Thirdly, DE materials with high environmental tolerance are expected. To promote applications of DEAs in harsh environments such as deep ocean, space, or underground, new DE materials which maintain their functionality in extreme temperatures, high moisture, and high pressure need to be developed. Finally, the safety issue resulting from high-voltage input is another limitation of DEAs. Although DEAs require a rather low operation current that is far below the human safety threshold, high voltage can pose a risk of electrical discharge around the actuators. From the perspective of material innovation, the dielectric constant of DE materials should be further increased to reduce the driving voltage. Different strategies such as incorporating organic dipole molecules, adding high-permittivity ceramic fillers, or introducing conductive nanofillers could be combined to achieve a high dielectric constant without sacrificing actuation performance.

The development of MDEAs is as important as material innovation of DEs, since it provides a promising way of improving the force, energy, and displacement outputs of DEAs without increasing the driving voltage. Conventional dry stacking methods which physically adhere DE films together, and wet stacking methods where an uncured DE film is deposited on a cured DE surface, have been widely explored and applied for fabrication of MDEAs. However, these methods are limited by poor bonding or low efficiency. A novel dry stacking method was recently reported, which shows high efficiency for fabrication of high-performance MDEAs and demonstrates great potential for large-scale manufacturing.

Nonetheless, many challenges still exist in the fabrication of MDEAs, and multilayer stacking methods should be further modified. These multilayer stacking methods should be carefully designed to be applicable for ultrathin DE films. It is well known that the high-voltage issue can be mitigated by using ultrathin DE films of <10 μm. However, manufacturing very thin DEs remains remarkably challenging, and processing them into multilayer stacks is even more difficult. The novel dry stacking method described above needs to be combined with thin-film processing techniques to ensure the uniformity of ultrathin DE films in MDEAs. In addition, it is important to improve the scalability of current multilayer stacking methods. The stacking processes should be optimized for compatibility with large-scale manufacturing, for example, roll-to-roll processing or continuous manufacturing such as 3D printing.

Acknowledgments

This work is supported by the National Natural Science Foundation of China (No. T229722).

Author contributions

Shengchao JIANG and Junbo PENG wrote the first draft of the manuscript. Lvting WANG helped to organize the manuscript. Ye SHI and Hanzhi MA revised and edited the final version. All authors approved the final manuscript.

Conflict of interest

Shengchao JIANG, Junbo PENG, Lvting WANG, Hanzhi MA, and Ye SHI declare that they have no conflict of interest.

References

Adeli Y, Owusu F, Nüesch FA, et al., 2023. On-demand crosslinkable bottlebrush polymers for voltage-driven artificial muscles. *ACS Applied Materials & Interfaces*, 15(16): 20410-20420. https://doi.org/10.1021/acsami.2c23026

Araromi OA, Conn AT, Ling CS, et al., 2011. Spray deposited multilayered dielectric elastomer actuators. *Sensors and Actuators A: Physical*, 167(2):459-467. https://doi.org/10.1016/j.sna.2011.03.004

Azoug A, Nevière R, Pradeilles-Duval RM, et al., 2014. Influence of crosslinking and plasticizing on the viscoelasticity of highly filled elastomers. *Journal of Applied Polymer Science*, 131(12):40392. https://doi.org/10.1002/app.40392

Brochu P, Stoyanov H, Niu X, et al., 2013. All-silicone prestrain-locked interpenetrating polymer network elastomers: free-standing silicone artificial muscles with improved performance and robustness. *Smart Materials and Structures*, 22(5):055022. https://doi.org/10.1088/0964-1726/22/5/055022

Chen YF, Zhao HC, Mao J, et al., 2019. Controlled flight of a microrobot powered by soft artificial muscles. *Nature*, 575(7782):324-329. https://doi.org/10.1038/s41586-019-1737-7

Chortos A, Hajiesmaili E, Morales J, et al., 2020. 3D printing of interdigitated dielectric elastomer actuators. *Advanced Functional Materials*, 30(1):1907375. https://doi.org/10.1002/adfm.201907375

Danner PM, Iacob M, Sasso G, et al., 2022. Solvent-free synthesis and processing of conductive elastomer composites for green dielectric elastomer transducers. *Macromolecular Rapid Communications*, 43(6):2100823. https://doi.org/10.1002/marc.202100823

Dickinson MH, Farley CT, Full RJ, et al., 2000. How animals move: an integrative view. *Science*, 288(5463):100-106. https://doi.org/10.1126/science.288.5463.100

Duduta M, Wood RJ, Clarke DR, 2016. Multilayer dielectric elastomers for fast, programmable actuation without prestretch. *Advanced Materials*, 28(36):8058-8063. https://doi.org/10.1002/adma.201601842

Duduta M, Hajiesmaili E, Zhao HC, et al., 2019. Realizing the potential of dielectric elastomer artificial muscles. *Proceedings of the National Academy of Sciences of the United States of America*, 116(7):2476-2481. https://doi.org/10.1073/pnas.1815053116

Dünki SJ, Ko YS, Nüesch FA, et al., 2015. Self-repairable, high permittivity dielectric elastomers with large actuation strains at low electric fields. *Advanced Functional Materials*, 25(16):2467-2475. https://doi.org/10.1002/adfm.201500077

Fu HB, Xu H, Liu Y, et al., 2022. A continuous spatial confining process towards high electrical conductivity of elastomer composites with a low percolation threshold. *Composites Science and Technology*, 218:109155. https://doi.org/10.1016/j.compscitech.2021.109155

Fu HB, Jiang Y, Lv J, et al., 2023. Multilayer dielectric elastomer with reconfigurable electrodes for artificial muscle. *Advanced Science*, 10(9):2206094. https://doi.org/10.1002/advs.202206094

Galantini F, Bianchi S, Castelvetro V, et al., 2013. Functionalized carbon nanotubes as a filler for dielectric elastomer composites with improved actuation performance. *Smart Materials and Structures*, 22(5):055025. https://doi.org/10.1088/0964-1726/22/5/055025

Guo YG, Liu LW, Liu YJ, et al., 2021. Review of dielectric elastomer actuators and their applications in soft robots. *Advanced Intelligent Systems*, 3(10):2000282. https://doi.org/10.1002/aisy.202000282

Guo YX, Qin QC, Han ZQ, et al., 2023. Dielectric elastomer artificial muscle materials advancement and soft robotic applications. *SmartMat*, 4(4):e1203. https://doi.org/10.1002/smm2.1203

Ha SM, Yuan W, Pei QB, et al., 2007. Interpenetrating networks of elastomers exhibiting 300% electrically-induced area strain. *Smart Materials and Structures*, 16(2):S280-S287. https://doi.org/10.1088/0964-1726/16/2/S12

Hajiesmaili E, Clarke DR, 2019. Reconfigurable shape-morphing dielectric elastomers using spatially varying electric fields. *Nature Communications*, 10(1):183. https://doi.org/10.1038/s41467-018-08094-w

Hajiesmaili E, Larson NM, Lewis JA, et al., 2022. Programmed shape-morphing into complex target shapes using architected dielectric elastomer actuators. *Science Advances*, 8(28):eabn9198. https://doi.org/10.1126/sciadv.abn9198

Han ZQ, Peng ZH, Guo YX, et al., 2023. Hybrid fabrication of prestrain-locked acrylic dielectric elastomer thin films and multilayer stacks. *Macromolecular Rapid Communications*, 44(15):2300160. https://doi.org/10.1002/marc.202300160

Huang YH, Xu ZW, Shi XH, et al., 2022. Study on the improved electromechanical properties of composited dielectric elastomer by tailoring three-dimensional segregated multi-walled carbon nanotube (MWCNT) network. *Composites Science and Technology*, 223:109424. https://doi.org/10.1016/j.compscitech.2022.109424

Iacob M, Verma A, Buchner T, et al., 2022. Slot-die coating of an on-the-shelf polymer with increased dielectric permittivity for stack actuators. *ACS Applied Polymer Materials*, 4(1):150-157. https://doi.org/10.1021/acsapm.1c01135

Jiang L, Zhou Y, Chen S, et al., 2018. Electromechanical instability in silicone-and acrylate-based dielectric elastomers. *Journal of Applied Polymer Science*, 135(9):45733. https://doi.org/10.1002/app.45733

Kovacs G, Düring L, Michel S, et al., 2009. Stacked dielectric elastomer actuator for tensile force transmission. *Sensors and Actuators A: Physical*, 155(2):299-307. https://doi.org/10.1016/j.sna.2009.08.027

Li ZY, Sheng MP, Wang MQ, et al., 2018. Stacked dielectric elastomer actuator (SDEA): casting process, modeling and active vibration isolation. *Smart Materials and Structures*, 27(7):075023. https://doi.org/10.1088/1361-665X/aabea5

Liu X, Yu LY, Nie Y, et al., 2019. Silicone elastomers with high-permittivity ionic liquids loading. *Advanced Engineering Materials*, 21(10):1900481. https://doi.org/10.1002/adem.201900481

Löwe C, Zhang X, Kovacs G, 2005. Dielectric elastomers in actuator technology. *Advanced Engineering Materials*, 7(5):361-367. https://doi.org/10.1002/adem.200500066

Mirvakili SM, Hunter IW, 2018. Artificial muscles: mechanisms, applications, and challenges. *Advanced Materials*, 30(6):1704407. https://doi.org/10.1002/adma.201704407

Ni YF, Yang D, Wei QG, et al., 2020. Plasticizer-induced enhanced electromechanical performance of natural rubber dielectric elastomer composites. *Composites Science and Technology*, 195:108202. https://doi.org/10.1016/j.compscitech.2020.108202

Niu XF, Stoyanov H, Hu W, et al., 2013. Synthesizing a new dielectric elastomer exhibiting large actuation strain and suppressed electromechanical instability without prestretching. *Journal of Polymer Science Part B: Polymer Physics*, 51(3):197-206. https://doi.org/10.1002/polb.23197

O'Halloran A, O'Malley F, McHugh P, 2008. A review on dielectric elastomer actuators, technology, applications, and challenges. *Journal of Applied Physics*, 104(7):071101. https://doi.org/10.1063/1.2981642

Pelrine R, Kornbluh R, Pei QB, et al., 2000a. High-speed electrically actuated elastomers with strain greater than

100%. *Science*, 287(5454):836-839. https://doi.org/10.1126/science.287.5454.836

Pelrine R, Kornbluh R, Kofod G, 2000b. High-strain actuator materials based on dielectric elastomers. *Advanced Materials*, 12(16):1223-1225. https://doi.org/10.1002/1521-4095(200008)12:16<1223::AID-ADMA1223>3.0.CO;2-2

Palmić TB, Slavič J, 2022. Single-process 3D-printed stacked dielectric actuator. *International Journal of Mechanical Sciences*, 230:107555. https://doi.org/10.1016/j.ijmecsci.2022.107555

Plante JS, Dubowsky S, 2006. Large-scale failure modes of dielectric elastomer actuators. *International Journal of Solids and Structures*, 43(25-26):7727-7751. https://doi.org/10.1016/j.ijsolstr.2006.03.026

Qiu Y, Zhang E, Plamthottam R, et al., 2019. Dielectric elastomer artificial muscle: materials innovations and device explorations. *Accounts of Chemical Research*, 52(2):316-325. https://doi.org/10.1021/acs.accounts.8b00516

Reitelshöfer S, Göttler M, Schmidt P, et al., 2016. Aerosol-jet-printing silicone layers and electrodes for stacked dielectric elastomer actuators in one processing device. Proceedings of SPIE 9798, Electroactive Polymer Actuators and Devices, article 97981Y. https://doi.org/10.1117/12.2219226

Ren ZJ, Kim S, Ji X, et al., 2022. A high-lift micro-aerial-robot powered by low-voltage and long-endurance dielectric elastomer actuators. *Advanced Materials*, 34(7):2106757. https://doi.org/10.1002/adma.202106757

Romasanta LJ, Hernández M, López-Manchado MA, et al., 2011. Functionalised graphene sheets as effective high dielectric constant fillers. *Nanoscale Research Letters*, 6(1):508. https://doi.org/10.1186/1556-276X-6-508

Romasanta LJ, Lopez-Manchado MA, Verdejo R, 2015. Increasing the performance of dielectric elastomer actuators: a review from the materials perspective. *Progress in Polymer Science*, 51:188-211. https://doi.org/10.1016/j.progpolymsci.2015.08.002

Sheima Y, Venkatesan TR, Frauenrath H, et al., 2023. Synthesis of polysiloxane elastomers modified with sulfonyl side groups and their electromechanical response. *Journal of Materials Chemistry C*, 11(22):7367-7376. https://doi.org/10.1039/D3TC00200D

Shi Y, Askounis E, Plamthottam R, et al., 2022. A processable, high-performance dielectric elastomer and multilayering process. *Science*, 377(6602):228-232. https://doi.org/10.1126/science.abn0099

Son J, Lee S, Bae GY, et al., 2023. Skin-mountable vibrotactile stimulator based on laterally multilayered dielectric elastomer actuators. *Advanced Functional Materials*, 33(23):2213589. https://doi.org/10.1002/adfm.202213589

Su S, He T, Yang H, 2023. 3D printed multilayer dielectric elastomer actuators. *Smart Materials and Structures*, 32(3):035021. https://doi.org/10.1088/1361-665X/acb677

Suresh JN, Arief I, Naskar K, et al., 2023. The role of chemical microstructures and compositions on the actuation performance of dielectric elastomers: a materials research perspective. *Nano Select*, 4(5):289-315. https://doi.org/10.1002/nano.202200254

Tan MWM, Thangavel G, Lee PS, 2019. Enhancing dynamic actuation performance of dielectric elastomer actuators by tuning viscoelastic effects with polar crosslinking. *NPG Asia Materials*, 11(1):62. https://doi.org/10.1038/s41427-019-0147-5

Tang C, Du BY, Jiang SW, et al., 2023. A review on high-frequency dielectric elastomer actuators: materials, dynamics, and applications. *Advanced Intelligent Systems*, in press. https://doi.org/10.1002/aisy.202300047

Tang DY, Zhang JS, Zhou DR, et al., 2005. Influence of $BaTiO_3$ on damping and dielectric properties of filled polyurethane/unsaturated polyester resin interpenetrating polymer networks. *Journal of Materials Science*, 40(13):3339-3345. https://doi.org/10.1007/s10853-005-0423-3

Tugui C, Serbulea MS, Cazacu M, 2019. Preparation and characterisation of stacked planar actuators. *Chemical Engineering Journal*, 364:217-225. https://doi.org/10.1016/j.cej.2019.01.150

Vatankhah-Varnoosfaderani M, Daniel WFM, Zhushma AP, et al., 2017. Bottlebrush elastomers: a new platform for freestanding electroactuation. *Advanced Materials*, 29(2):1604209. https://doi.org/10.1002/adma.201604209

Vudayagiri S, Zakaria S, Yu LY, et al., 2014. High breakdown-strength composites from liquid silicone rubbers. *Smart Materials and Structures*, 23(10):105017. https://doi.org/10.1088/0964-1726/23/10/105017

Wang H, Tan MWM, Poh WC, et al., 2023. A highly stretchable, self-healable, transparent and solid-state poly (ionic liquid) filler for high-performance dielectric elastomer actuators. *Journal of Materials Chemistry A*, 11(26):14159-14168. https://doi.org/10.1039/D3TA01954C

Yin LJ, Zhao Y, Zhu J, et al., 2021. Soft, tough, and fast polyacrylate dielectric elastomer for non-magnetic motor. *Nature Communications*, 12(1):4517. https://doi.org/10.1038/s41467-021-24851-w

Zhang FX, Li TF, Luo YW, 2018. A new low moduli dielectric elastomer nano-structured composite with high permittivity exhibiting large actuation strain induced by low electric field. *Composites Science and Technology*, 156:151-157. https://doi.org/10.1016/j.compscitech.2017.12.016

Zhang H, Düring L, Kovacs G, et al., 2010. Interpenetrating polymer networks based on acrylic elastomers and plasticizers with improved actuation temperature range. *Polymer International*, 59(3):384-390. https://doi.org/10.1002/pi.2784

Zolfagharian A, Kouzani AZ, Khoo SY, et al., 2016. Evolution of 3D printed soft actuators. *Sensors and Actuators A: Physical*, 250:258-272. https://doi.org/10.1016/j.sna.2016.09.028